

# Oxygen in the Very Early Galaxy<sup>1</sup>

Garik Israelian, Rafael Rebolo<sup>2</sup>, Ramón J. García López<sup>3</sup>

Instituto de Astrofísica de Canarias, E-38200 La Laguna, Tenerife, Spain

Piercarlo Bonifacio, Paolo Molaro

Osservatorio Astronomico di Trieste, Via G. B. Tiepolo 11, I-34131 Trieste, Italy

Gibor Basri

Astronomy Department, University of California, Berkeley, California 94720, USA

and

Nataliya Shchukina

Main Astronomical Observatory, National Academy of Sciences, 03680 Kyiv-127, Ukraine

arXiv:astro-ph/0101032v1 3 Jan 2001

---

<sup>1</sup>Based on data collected at the KeckI, VLT and William Herschel telescopes

<sup>2</sup>Consejo Superior de Investigaciones Científicas, Spain

<sup>3</sup>Departamento de Astrofísica, Universidad de La Laguna, E-38071 La Laguna, Tenerife, Spain

## ABSTRACT

Oxygen abundances in a sample of ultra-metal-poor subdwarfs have been derived from measurements of the oxygen triplet at 7771–5 Å and OH lines in the near UV performed in high-resolution and high signal-to-noise spectra obtained with WHT/UES, KeckI/HIRES, and VLT/UVES. Our Fe abundances were derived in LTE and then corrected for NLTE effects following Thévenin & Idiart (1999). The new oxygen abundances confirm previous findings for a progressive linear rise in the oxygen-to-iron ratio with a slope  $-0.33 \pm 0.02$  from solar metallicity to  $[\text{Fe}/\text{H}] \sim -3$ . A slightly higher slope would be obtained if the Fe NLTE corrections were not considered. Below  $[\text{Fe}/\text{H}] = -2.5$  our stars show  $[\text{O}/\text{Fe}]$  ratios as high as  $\sim 1.17$  (G64-12), which can be interpreted as evidence for oxygen overproduction in the very early epoch of the formation of the halo, possibly associated with supernova events with very massive progenitor stars. We show that the arguments against this linear trend given by Fulbright & Kraft (1999), based on the LTE Fe analysis of two metal-poor stars cannot be sustained when an NLTE analysis is performed. We discuss how the Fulbright & Kraft (1999) LTE ionization balance of Fe lines underestimates the gravity of the very metal-poor star BD +23°3130 ( $[\text{Fe}/\text{H}] = -2.43$ ) and how this leads to an underestimation of the oxygen abundance derived from the forbidden line. Gravities from *Hipparcos* appear to be in good agreement with those determined in NLTE, giving higher values than previously assumed, which reduces the discrepancies between the oxygen abundances determined from OH, triplet, and forbidden lines. Using 1-D models our analysis of three oxygen indicators available for BD +23°3130 gives consistent abundances within 0.16 dex and average  $[\text{O}/\text{Fe}]$  ratio of 0.91. The high oxygen abundances at very low metallicities do not pose a problem to theoretical modeling since there is a range of parameters in the calculations of nucleosynthesis yields from massive stars at low metallicities that can accommodate our results.

*Subject headings:* Galaxy: evolution — nuclear reactions, nucleosynthesis, abundances — stars: abundances — stars: late-type — stars: Population II

## 1. Introduction

The halo dwarfs contain fossilized records of the early Galaxy’s composition. The chemical composition of their atmospheres is not altered by any internal mixing and provides a unique opportunity to constrain models of the chemical evolution of the Galaxy. Oxygen is a key element in this scheme. It is produced in the interiors of massive stars by hydrostatic burning and returned to the interstellar medium (ISM) when the stars explode as Type II supernovae.

There have been numerous investigations of the oxygen abundances in halo stars. Despite considerable observational effort the trend of the  $[\text{O}/\text{Fe}]$ , ( $[\text{O}/\text{Fe}] = \log (\text{O}/\text{Fe})_{\star} - \log (\text{O}/\text{Fe})_{\odot}$ ), ratio in the halo is still unclear. Analysis of the forbidden line  $[\text{O I}]$  6300 Å in giants shows a *plateau* with  $[\text{O}/\text{Fe}] = 0.4\text{--}0.5$  in the metallicity domain  $-3 < [\text{Fe}/\text{H}] < 0$  (Barbuy 1988; Kraft et al. 1992). On the other hand, results based on the near-IR triplet at 7771–5 Å in unevolved subdwarfs (Abia & Rebolo 1989; Tomkin et al., 1992; King & Boesgaard 1995; Cavallo, Pilachowski, & Rebolo 1997) point towards increasing  $[\text{O}/\text{Fe}]$  values with decreasing  $[\text{Fe}/\text{H}]$ , reaching a ratio  $\sim 1$  for stars with  $[\text{Fe}/\text{H}] \sim -3$  (but see Carretta, Gratton, & Sneden 2000) and suggesting a higher production of oxygen during the early life of the Galaxy. More recent NLTE analyses of the triplet in metal-poor stars have been performed by Mishenina et al. (2000), Carretta et al. (2000), and Takeda et al. (2000) showing a range for the NLTE abundance corrections.

Studies based on OH lines in the near-UV (Bessell, Sutherland, & Ruan 1991; Nissen et al. 1994) concluded that  $[\text{O}/\text{Fe}]$  is constant at  $[\text{Fe}/\text{H}] < -1$ , in agreement with results based on the forbidden lines in giants. Contrary to this, oxygen abundances derived from near-UV OH lines for 24 metal-poor stars by Israelian, García López, & Rebolo (1998) show that the  $[\text{O}/\text{Fe}]$  ratio increases from 0.6 to 1 between  $[\text{Fe}/\text{H}] = -1.5$  and  $-3$  with a slope of  $-0.31 \pm 0.11$ . These new abundances derived from low-excitation OH lines agreed well with those derived from high-excitation lines of the O I triplet. The comparison with oxygen abundances derived using O I data from Tomkin et al. (1992) showed a mean difference of  $0.00 \pm 0.11$  dex for the stars in common. Boesgaard et al. (1999a), using high-quality Keck spectra of many metal-poor stars in the near UV, found a very good agreement with the results obtained by Israelian et al. (1998), and basically the same dependence of  $[\text{O}/\text{Fe}]$  versus metallicity. The mean difference in oxygen abundance for ten stars in common is  $0.00 \pm 0.06$  dex when the differences in stellar parameters are taken into account.

The linear trend of the  $[\text{O}/\text{Fe}]$  ratio found in the analysis of OH and triplet lines has been recently questioned by Fulbright & Kraft (1999) (hereafter FK) who obtained low values of  $[\text{O}/\text{Fe}]$  for two metal-poor subgiants using the  $[\text{O I}]$  lines. In the present paper we discuss their claims in the light of a NLTE analysis of Fe lines and report on new detections of the OH and O I triplet lines in several unevolved ultra-metal-poor stars with  $[\text{Fe}/\text{H}] \leq -2.5$ .

## 2. The Observations

The spectroscopic observations of several metal-poor subdwarfs were carried out in different runs using the 4.2 m WHT/UES (La Palma), the 10 m KeckI/HIRES (Hawaii), and the 8.2m VLT Kueyen/UVES (Paranal). See the observing log in Table 1. All observations with WHT/UES were obtained using the E31 grating. In the first run (1996) we observed BD +03°740, BD +23°3130, and G4-37 using a 1''1 arcsec slit and a TEK CCD (1024 × 1024 pixel<sup>2</sup> giving a dispersion of 0.06 Å pix<sup>-1</sup>). The same configuration but a CCD SITE1 (2148 × 2148 pixel<sup>2</sup> detector giving a dispersion of 0.076 Å pix<sup>-1</sup>) was used to obtain a few images of G64-37 in 1997. This star, together with G268-32, was observed in 1999 with the same configuration and a slit width of 3''0. All the WHT/UES images were reduced using standard IRAF routines. Normalized flats created for each observing night were used to correct the pixel-to-pixel variations and a ThAr lamp was used to find a dispersion solution. Observations with the 2.5 m Nordic Optical Telescope (NOT) and the SOFIN high-resolution spectrograph were used only to study the Fe abundance of some of the targets. A resolving power of  $\sim 30\,000$  has been achieved with the short camera (350 mm focal length, third camera) with a slit width of  $\sim 1''0$ . The CCD used in this run was a 1152 × 770 pixel<sup>2</sup> EEV.

The Keck observations were carried out with the HIRES spectrograph and the TEK 2048 × 2048 pixel<sup>2</sup> CCD, which has been its only detector to date. We did not bin the chip, so the resolution is about 60 000 with the 1''1 slit. The slit length was 14''0, allowing good sky subtraction. The seeing was slightly worse than 1''0. Standard calibration exposures and procedures were used to reduce the data. A red wavelength setting was used to observe the oxygen triplet lines; this setting has incomplete coverage of the echelle format.

The UVES data for G271-162, G275-4, and LP 815-43 were obtained during the commissioning of the instrument, while the data for G64-12 were obtained during the science verification. UVES has two arms: blue and red. In the blue arm the detector is an EEV of 4096 × 2048 square pixels of size 15 μm. In the red arm the detector is a mosaic of two CCDs: an EEV identical to that of the blue arm and an MIT with the same number of pixels and pixel size as the EEV. The data for G271-162 consist of four spectra in the red arm centered at 7100 Å with a slit width of 0''3 which results in a resolution of  $\approx 110\,000$ . These spectra are the same ones used by Nissen et al. (2000) although they have been independently reduced by us. The O I triplet falls on the MIT CCD. The spectra of G271-162 were trailed along the slit. For G275-4 the data consist of three spectra taken with dichroic #1, the blue arm spectra are all centered at 3460 Å, while the red arm spectra are centered at 5400 Å, 5800 Å, and 8600 Å. The only red spectrum used in this paper is that centered at 8600 Å, in which the triplet (not detected) falls on the EEV CCD. The slit width was 1''0 both for the red and the blue arm. For LP 815-43 we also have three spectra, but taken in the blue arm only (no dichroic). Two spectra were taken with a slit width of 1''1 and one with a slit width of 0''8. In order to combine the spectra, the higher-resolution spectrum has been degraded to lower resolution by convolving with a Gaussian of appropriate FWHM. For G64-12 the data consist of four blue and four red spectra observed with dichroic #1. All blue arm spectra

are centered at 3460 Å. Two of the red arm spectra are centered at 5800 Å and two at 8600 Å. The triplet falls on the EEV CCD of these latter frames. The slit width was always 0.8" for both arms. The UVES spectra have been background-subtracted, filtered for cosmic rays, flat-fielded, extracted, and wavelength-calibrated using the echelle context of MIDAS.

Our detections of the oxygen triplet are presented in Figure 1. We have detected for the first time the oxygen triplet in G268-32, G4-37, and G271-162. We also report on a possible detection of the bluest line of the triplet with an equivalent width of 6 mÅ in G64-12. Unfortunately the line is located at the edge of the order (which in addition suffers strong fringing) and therefore we cannot give much weight to this detection. The presence of the triplet is confirmed in BD +03°740 (the strongest line was already measured by Tomkin et al. 1992) and in BD +23°3130. In the latter case we have detected all three lines of the triplet and measured equivalent widths of  $7 \pm 2$ ,  $5 \pm 2$ , and  $3 \pm 2$  mÅ, in good agreement with the observations of Mishenina et al. (2000).

We have achieved the detection of OH lines in the near-UV spectra of three ultra-metal-poor subdwarfs observed during VLT/UVES commissioning and science verification. Most of the unblended OH lines carefully selected and studied by Israelian et al. (1998) have been unambiguously detected in the spectra of G64-12, G275-4 (CD–24°17504), and LP815-43. Some of these lines are shown in Figure 2. The S/N in the continuum is given in Table 1. The quality of these spectra allows us to perform spectral synthesis and to determine the abundance of oxygen.

### 3. Spectral synthesis, stellar parameters and abundances

The LTE spectrum synthesis program WITA (Pavlenko 1991) and ATLAS9 model atmospheres (Kurucz 1992) were employed in the present study. However, in this paper we have also performed computations with the MOOG code (Snedden 1973) in order to be sure that there are no systematic differences connected with the use of different spectrum synthesis packages. We found that in all cases considered the agreement between WITA and MOOG was very good. The solar oxygen abundance used for the differential analysis of OH lines was  $\log \epsilon(\text{O})=8.93$  (on the customary scale in which  $\log \epsilon(\text{H})=12$ ) according to Anders & Grevesse (1989). For the triplet and [O I] we used the solar abundances  $\log \epsilon(\text{O})=8.98$  and  $\log \epsilon(\text{O})=8.90$ , respectively, derived by Israelian et al. (1998). The oscillator strengths of the O I triplet and iron lines were taken from Tomkin et al. (1992) and O’Brian et al. (1991), respectively. Effective temperatures ( $T_{\text{eff}}$ ) for our stars were estimated using the Alonso, Arribas, & Martínez-Roger (1996) and Carney (1983) calibrations versus  $V-K$  colors, and cover a wide range of spectral types and metal content. The  $K$ -band photometry was kindly provided by A. Alonso prior the publication of the data (A. Alonso, private communication). Our final  $T_{\text{eff}}$  is an average value obtained from these two calibrations. Since there are no accurate *Hipparcos* parallaxes available for our targets (except for BD +23°3130) we estimated surface gravities by comparing Strömberg  $b-y$  and  $c_1$  indices with synthetic ones generated using the corresponding filter transmissions and a grid of ATLAS9 blanketed model atmosphere fluxes. For BD +23°3130 we obtained  $\log g = 3.05 \pm 0.25$  from the *Hipparcos* parallax

(Perryman et al. 1997) following the recipe given in Allende Prieto et al. (1999) and assuming an IRFM based  $T_{\text{eff}}=5130\pm150$  K from Israelian et al. (1998). The final stellar parameters of our targets (except BD +23°3130, which will be treated separately in section 5), along with a representative selection of parameters reported by different authors in the literature (by no means exhaustive), are listed in Table 2. It can be seen that our parameters are not very different from those reported in different sources.

For the present analysis we used the same model atmospheres than Israelian et al. (1998) provided by Kurucz (1992, private communication) and built with the approximate overshooting option switched on (note that a typographic error mistakenly stated that the models used in Israelian et al. had no overshooting). The differences between models with and without convective overshooting have been discussed by Castelli, Gratton & Kurucz (1997) and Molaro, Bonifacio & Primas (1995). We have explicitly computed the effects of overshooting versus non-overshooting in the formation of OH, [O I], oxygen triplet and the Fe lines listed in Tables 3 and 4 for a range of model parameters, and find that the differences induced in the [O/Fe] ratios by the two types of models are less than 0.05 dex.

The LTE metallicities of our targets have been estimated using a sample of unblended Fe I lines listed in Tables 3 and 4 with accurately known oscillator strengths. The equivalent widths of the iron lines were measured in the spectra listed in Table 1. For only one star, G271-162, we took the measurements from the literature (Zhao & Magain 1990). NLTE estimates for the Fe abundances of our stars have been made using the work of Thévenin & Idiart (1999). In their Fig. 9 we can see NLTE corrections for Fe abundances in metal-poor stars as a function of  $[\text{Fe}/\text{H}]_{\text{LTE}}$ . In a first approximation we can see that these corrections mostly depend on metallicity and there is no clear dependence on the effective temperatures and gravities. So, we have fitted a third order polynomial to the data provided in their Table 1, suitably reproducing the trend seen in their figure. The resulting polynomial fit is

$$[\text{Fe}/\text{H}]_{\text{NLTE}} - [\text{Fe}/\text{H}]_{\text{LTE}} = -0.001 - 0.204 \times [\text{Fe}/\text{H}]_{\text{LTE}} - 0.052 \times ([\text{Fe}/\text{H}]_{\text{LTE}})^2 - 0.006 \times ([\text{Fe}/\text{H}]_{\text{LTE}})^3$$

We have used this function to estimate the  $[\text{Fe}/\text{H}]_{\text{NLTE}}$  for our stars and listed the resulting values in Table 7.

All our targets except two (BD +03°740 and BD +23°3130) are relatively distant, and their colors could be affected by interstellar reddening. Unfortunately, the reddening values of our targets are very uncertain and we have decided not to consider them. The reddening correction will increase the  $T_{\text{eff}}$  values of our stars which will increase the oxygen abundances derived from the OH and [O I] lines and diminish the abundance derived from the triplet.

In Table 3 we present oxygen LTE abundances from the parameters given in Table 2. It is well known that the oxygen abundance in metal-poor subdwarfs derived from the O I is slightly

sensitive to NLTE effects (Kiselman 1993, Takeda 1995). Tomkin et al. (1992) estimate NLTE corrections of less than 0.1 dex for hot subdwarfs with  $T_{\text{eff}}$  around 6200 K. Our stars have these temperatures, and corrections will be of this order or smaller due to the weakness of our triplet lines. However, larger NLTE corrections could be necessary if the hydrogen collision rates employed by Tomkin et al. (1992) were overestimated, as suggested by Fleck et al. (1991) and Belyaev et al. (1999).

Oxygen abundances in G275-4, G64-12, and LP815-43 were derived by fitting the OH lines (see Figure 3) in the near-UV with oscillator strengths adjusted to reproduce the solar spectrum ( $\log gf_{\text{ad}}$ , used by Israelian et al. 1998). The adjustments were most probably due to imprecise  $gf$ -values of other weak lines blended with OH. It is well known that the line lists available in the literature are not complete and/or perfect and Israelian et al. (1998) tried to empirically minimize the effect they could have by adjusting the  $gf$ 's of the OH. It is possible that some of these blended lines will disappear in metal-poor stars (especially if they belong to one of the Fe-group elements) causing a systematic difference in oxygen abundance. However, this will not affect our [O/H] ratios by more than 0.1 dex.

The results for each star and each line are listed in Table 4. In this table we also provide theoretical  $\log gf_{\text{th}}$  values derived from new transition probabilities recently computed by Gillis et al. (2000). When computing new theoretical  $gf$  values from the transition probabilities provided by Gillis et al. (2000), we found two mistakes in Table 2 of Israelian et al. (1998). The values of  $\log gf_{\text{th}}$  for the lines 3167.169 and 3186.084 Å were not correct. The correct values of  $\log gf_{\text{th}}$  must be  $-1.540$  and  $-1.830$  for the 3167.169 and 3186.084 Å lines, respectively. It can be seen from Table 4 and Table 2 of Israelian et al. (1998) that these new  $gf$  values of Gillis et al. (2000) are almost identical to those of Goldman & Gillis (1981) and that the maximum difference between the  $\log gf$  values adjusted to reproduce the solar OH lines and the new theoretical ones is  $-0.24$  dex, while the mean difference correction is  $-0.11$  dex. We note that the most accurate measurement is achieved in G64-12 where the error in oxygen abundance due to the continuum placement for individual OH lines is as small as 0.2 dex (see Figure 3). However, in the case of G275-4 these errors may reach 0.35 dex. We regard the clear detection of OH lines in G64-12 as an important confirmation of the linear trend of [O/Fe] versus [Fe/H]. Indeed, even if we suppose that the near-UV continuum is not well determined and that the  $gf$  values of the OH lines are underestimated, the [O/Fe] ratio in G64-12 will decrease because of this effect by 0.1 at most. In addition, assuming for this star the smallest effective temperature reported in the literature ( $T_{\text{eff}} = 6197$  K; Table 2) would bring the [O/H] ratio down by another 0.2 dex. In any case we would obtain a value of [O/Fe]  $> 0.9$ .

#### 4. How reliable are the abundances derived from the O I triplet, OH, and [O I] ?

Recently, Mishenina et al. (2000) performed a NLTE analysis of the O I triplet to re-derive oxygen abundances for a sample of 38 metal-poor stars from the literature. They confirmed earlier

results (Abia & Rebolo 1989; Tomkin et al. 1992; Kiselman 1993) indicating that the mean value of the NLTE correction in unevolved metal-poor stars is typically 0.1 dex and never exceeds 0.2 dex. Mishenina et al. found the same linear trend as Israelian et al. (1998) and Boesgaard et al. (1999a) from the OH lines and confirmed that oxygen abundances do not show any trend with  $T_{\text{eff}}$  or  $\log g$  (Boesgaard et al. 1999a). Furthermore, Asplund et al. (1999) showed that the O I triplet is not affected by 3D effects, convection, or small-scale inhomogeneities in the stellar atmosphere. In addition, oxygen abundances derived from this triplet are not significantly affected by chromospheric activity either, showing that the O I triplet provides reliable oxygen abundances in metal-poor dwarfs. Preliminary calculations by Asplund et al. (1999) and Asplund (2000) show that 3D models give stronger OH lines than those computed with 1D models which would decrease the oxygen abundances found in the present paper. However, first the precise value of 3D corrections will consistently require a revision of the stellar parameters according to the same models and, second, Fe abundances including NLTE effects should be obtained with these models in order to properly estimate the [O/Fe] ratio.

Carretta et al. (2000) performed an independent analysis of 32 metal-poor stars hotter than 4600 K using the triplet, and provide LTE and NLTE oxygen abundances that are significantly lower than those found in previous works. A preliminary attempt to understand the reasons for this discrepancy can be made by looking in detail into their most metal-poor star (BD +03°740, [Fe/H] = -2.66), where a surprisingly low oxygen abundance ([O/Fe] = 0.38) is claimed. A recent study of stellar parameters based on the NLTE analysis of iron lines (Thévenin & Idiart 1999), gives a lower effective temperature by 140 K (actually very similar to the temperature we have derived in this paper) and a higher gravity by 0.3 dex (also very similar to ours) than the values adopted by Carretta et al., for this star. Using the Thévenin & Idiart parameters we obtain an LTE oxygen abundance 0.4 dex higher than that found by Carretta et al. (i.e., [O/Fe]<sub>LTE</sub> = 1.05), and for a star with these parameters the NLTE correction to the oxygen abundance is of the order of 0.05 dex (Mishenina et al. 2000; Tomkin et al. 1992), much lower than the 0.25 dex value used by Carretta et al. We therefore arrive at a value [O/Fe]<sub>NLTE</sub> ~ 1.0, in good agreement with the OH determination by Boesgaard et al. (1999a). The oxygen abundances derived by Carretta et al., are computed using the gravities from Gratton, Carretta, & Castelli (1996), whose values come from an LTE Fe ionization balance. As a matter of fact, Gratton et al. (1996) remark that their gravities are considerable lower (see their Figure 2) than those derived from the color-magnitude diagram. They also suggest that this discrepancy may be due to a NLTE effect.

The OH lines may be affected by the UV “missing opacity”, as discussed by Balachandran & Bell (1998). Allende Prieto & Lambert (2000) found a good agreement between effective temperatures obtained from the infrared flux method (IRFM) and from the near-UV continuum for stars with  $4000 \leq T_{\text{eff}} \leq 6000$  K when accurate *Hipparcos* gravities are used. This also agrees with our good reproduction of the near-UV spectral region and indicates that the model atmospheres used provide an adequate description of the near-UV continuum-forming region. In any case, even if a poorly understood opacity problem existed as described by Balachandran &

Bell, it would have a minor effect on the OH results since most of the stars in the samples of Israelian et al. (1998), and Boesgaard et al. (1999a), are hotter than the Sun and very metal-poor. It must be mentioned that the OH lines employed by Israelian et al. (1998) and Boesgaard et al. (1999a) to study the most metal-poor stars in their samples are from the (0,0) band, where the corrections to theoretical  $gf$  values are not large. Considering the list used by Israelian et al. (1998), we note that only for 3 lines out of 12 these corrections exceed 0.15 dex. The same is true for the list employed by Boesgaard et al. (1999a), who used  $gf$  values from Nissen et al. (1994). The corrections applied to their  $gf$  values are only 0.15 dex. Thus, corrections to oxygen abundances due to opacity problems should not exceed 0.15 dex for the stars used in the present study. This will not change the  $[O/Fe]$  vs.  $[Fe/H]$  trend significantly.

The forbidden line of oxygen is sensitive to the stellar gravity. Israelian et al. (1998) synthesized this line for four dwarfs adopting the same set of stellar parameters as in the OH analysis, the  $gf$  value given by Lambert (1978), and the equivalent widths provided in the literature for the  $\lambda$  6300 Å line. The estimated abundances were in good agreement with those derived from OH when gravities from *Hipparcos* are used. This strongly suggests that a reliable gravity scale may indeed be the key to explaining the discrepancies in oxygen abundances from forbidden and permitted lines in unevolved metal-poor stars. This conclusion is supported by Mishenina et al. (2000), who also found good agreement between  $[OI]$  and the triplet for three unevolved halo stars in their sample. Nevertheless, all stars with measured  $[OI]$  in Mishenina et al. (2000) and Israelian et al. (1998) have  $[Fe/H] > -1.4$  and leave open the possibility that differences between oxygen indicators may appear at much lower metallicities. Indeed, FK claimed that there was inconsistent results for the two metal-poor stars BD +23°3130 and BD +37°1458 using stellar parameters derived from an LTE analysis of iron lines. These objects were also considered by Israelian et al. (1998) and Boesgaard et al. (1999a) (only BD +37°1458 in the latter case). While FK's conclusions for BD +37°1458 do not challenge the linear trend in  $[O/Fe]$ , their results for BD +23°3130 are claimed to be inconsistent with those from OH lines. However, we argue in the next section that this discrepancy cannot be sustained when a critical analysis of the uncertainties involved in the determination from the forbidden line is performed.

It is often claimed in the literature that the abundances derived from the forbidden lines are more reliable than those from the triplet and OH. The authors of this statement refer mainly to the fact that the forbidden lines at 6300 and 6363 Å are not affected by NLTE effects and are less sensitive to the uncertainties in  $T_{\text{eff}}$ . However, results based on the forbidden lines should be interpreted with caution. Figure 4 demonstrates that very small errors in the equivalent widths (EW) of the forbidden line at 6300 Å may have a dramatic effect on the derived oxygen abundances. Very high signal-to-noise (S/N) ratio is required in order to minimize this uncertainty; condition which is normally not satisfied in most of the studies based on the forbidden line. For example, Barbuy (1988) used data with a signal-to-noise ratio of 90 and  $R \sim 40.000$  in order to derive the oxygen abundance from the forbidden line (EW = 4 mÅ) in the most metal-poor giant in her sample: BD -18°5550 ( $[Fe/H] = -3$ ). Note that a S/N~90 optimistically implies about

$\pm 2 \text{ m}\text{\AA}$  of uncertainty (at  $1\text{-}\sigma$  level) in the EW according to Cayrel’s formulae (Cayrel 1988), which introduces an uncertainty in the derived abundance of oxygen larger than  $+0.18$  and  $-0.3$  dex (Figure 4). To this error (which comes from measuring only one weak line) we must add the systematic errors due to the uncertainties in gravity (note that Barbuy 1988 used only 3 lines of each Sc I and Sc II to estimate the gravity) and effective temperature. This makes the total error from the [O I] line large.

Another problem is that the gravities of metal-poor giants derived from the LTE Fe analysis are most probably underestimated because of the neglect of NLTE effects. This effect is already proven to exist in metal-poor dwarfs (Thévenin & Idiart 1999) and also in a subgiant (BD +23°1330, this study). It has been argued (Thévenin & Idiart 1999; Gratton et al. 1996) that this effect also operates in metal-poor giants. Work is in progress to study NLTE effects on Fe in several metal-poor giants and our preliminary results indicate that corrections to gravities derived from the LTE analysis of Fe can indeed be as large as  $+0.5$  dex. We also note that recently Takeda et al. (2000) proposed that the [O I] lines in metal-poor giants may suffer some filling in emission that leads to the weakening of the absorption lines. This possibility has been noticed by Langer (1991), who proposed that the emission from the surrounding nebulosity, formed from the mass ejected in the post-RGB phase, may account for the observed weakness of the forbidden lines. The fact that some giants such as HD 115444 show [O/Fe] about 0.3 dex larger (Westin et al. 2000) than “expected” from the *plateau* ([O/Fe]  $\sim 0.4$ ) supports this idea. This is also consistent with the fact that there is no discrepancy between [O I], O I, and OH in several unevolved dwarfs.

## 5. The particular case of BD+23°3130

The analysis carried out by FK is based on gravities derived from LTE Fe ionization balance of these subgiants where the NLTE effects are strong. In general, NLTE effects play a dominant role in very metal-poor stars due to a decrease in electron density. Collisions with free electrons no longer dominate the kinetic equilibrium as they do in the stars of solar composition, and this leads to significant deviations from LTE. Another consequence of the metal deficiency is an appreciable weakening in UV blanketing. Both effects lead to a large depletion of the Fe I atoms affecting the equivalent widths and central depths of spectral lines (Shchukina & Trujillo Bueno 2000). In a recent paper, Allende Prieto et al. (1999) have shown that gravities derived using LTE analyses of iron in metal-poor stars do not agree with the gravities inferred from accurate *Hipparcos* parallaxes, which casts a shadow over oxygen abundance analyses of very metal-poor stars based on gravities derived from the LTE Fe ionization balance. They find that gravities are systematically underestimated when derived from ionization balances, and that upward corrections of 0.5 dex or even higher can be required at metallicities similar to those of our stars. We remark here that any underestimation of gravities will also strongly underestimate the abundances inferred from the forbidden and triplet lines. The abundances derived from OH will be affected as well but in the opposite direction. Thévenin & Idiart (1999) derived gravity corrections of up to 0.5 dex

with respect to LTE values, for the case of stars with  $[\text{Fe}/\text{H}] \sim -3.0$ . They have shown that NLTE effects are important in determining stellar parameters from iron ionization balance.

It has been established (see Rutten 1988, and references therein) that a strong overionization of neutral iron in metal-poor stars leads to the systematic difference in abundances determined from the Fe I and Fe II lines. This difference increases with decreasing metallicity. For the Fe II lines NLTE effects are found to be unimportant. The NLTE modeling predicts a dependence of the NLTE abundance corrections of Fe I lines on the lower excitation potential ( $\chi$ ). The corrections are particularly large for the low-excitation Fe I lines. Empirical determinations by Ruland et al. (1980), Magain (1988) and Magain & Zhao (1996) support this conclusion. The NLTE abundance corrections in the Sun are in the range 0.02–0.1 dex, while in the main-sequence stars later than type A they can reach 0.3–0.4 dex.

Taking the above into account, we evaluate the extent to which NLTE effects could influence the determination of the stellar parameters of BD + 23°3130.

## 5.1. NLTE analysis

### 5.1.1. The models and the NLTE solution

Our study is based on horizontally homogeneous models of LTE atmospheres in hydrostatic equilibrium. The grid of interpolated ATLAS9 models is used to perform NLTE computations spanning the following range of atmospheric parameters:  $4800 \leq T_{\text{eff}} \leq 5130$  K,  $2 \leq \log g \leq 3$ , and  $-3 < [\text{Fe}/\text{H}] < -2.5$ . Our NLTE stellar parameter analysis is based on the usual assumptions: i) iron abundances used to fit EWs of Fe I and Fe II lines to observed ones have to be independent of excitation potential of the lower level  $\chi$ ; ii) the iron abundances have to be independent on the line strengths; namely, the stronger Fe I lines have on average to give the same abundance as the weaker ones; iii) the average abundances obtained from Fe I and Fe II lines have to be equal.

The theoretical EWs of the Fe I and Fe II lines were computed using the formal solution of the radiative transfer equation. NLTE departure coefficients were found from the self-consistent solution of the kinetic and radiative-transfer equations using a new NLTE code, NATAJA (see for details Shchukina & Trujillo Bueno 1998; Shchukina & Trujillo Bueno 2000). Here it is enough to mention that we employed novel and effective iterative multilevel transfer methods and formal solvers that are capable of handling hundreds of transitions efficiently and make feasible 2D and 3D multilevel modeling (Auer, Fabiani Bendicho, & Trujillo Bueno 1994, Trujillo Bueno & Fabiani Bendicho 1995). Our Fe I + Fe II atomic model takes into account a multiplet structure and includes over 250 levels and 500 UV, optical, and IR transitions including the regime near Fe I continuum. The Fe I term diagram is, in fact, complete up to  $\chi \approx 5.7$  eV. At higher energies it contains about 50% of the terms identified by Nave et al. (1994). The Fe II diagram is very similar to the atomic model of Gigas (1986). It contains only the lowest terms with  $\chi < 5.9$  eV and 25

strong transitions (see Shchukina & Trujillo Bueno 1998, 2000).

### 5.1.2. Spectral lines selected for the analysis

Notwithstanding such a comprehensive atomic model it contains only 21 lines from the list of Fe I lines observed and measured in the spectrum of BD + 23°3130 by FK. All of them except one line cluster into a narrow  $\chi$  range between 2 and 3 eV. We marked them in Figures 5 and 6 by large unfilled circles. The only line that is outside the range ( $\lambda 7511.02 \text{ \AA}$ ) has  $\chi = 4.16 \text{ eV}$ .

This selection effect prevents us from using the Fe I abundance versus  $\chi$ -trend as a criterion of correctness of the stellar parameters. To avoid this shortcoming we tried to extend our line list to larger  $\chi$ -samples. According to FK, LTE synthesis of the 58 Fe I lines for the atmospheric model with parameters derived by these authors ( $T_{\text{eff}} = 4850$ ,  $\log g = 2$ , and  $\log \epsilon = 4.69$ ) produces very good agreement with observations (the standard deviation,  $\sigma$ , is only 0.04 dex). If we assume that these stellar parameters reproduce both the EWs from FK, and that such modeling of Fe I lines is correct not only for their observed list of Fe I lines but also for other Fe I lines located in the same wavelength region (4000–8000  $\text{\AA}$ ), then we can consider synthetic LTE equivalent widths of the latter lines as “observed” ones. Following this idea we have selected from our atomic model 98 Fe I lines and calculated their LTE equivalent widths using the model atmosphere with stellar parameters obtained by FK. Furthermore, these equivalent widths, ranging from 1.5 to 80 m $\text{\AA}$ , are considered as “quasi-observations”. The wavelengths of these Fe I lines, their  $\chi$ -values, and oscillator strengths are listed in Table 5. Note that these lines are distributed rather uniformly with  $\chi$ . In addition to the line cluster between 2 and 3 eV the new set contains 13 Fe I lines with  $\chi < 2 \text{ eV}$ , 27 lines in the range 3–3.8 eV and 17 lines with  $\chi > 3.8 \text{ eV}$ . Using our list of Fe lines we obtain with the stellar parameters of FK the same LTE Fe abundance claimed in their paper. It is interesting to note that everywhere in our figures, abundances for the aforementioned high-excitation Fe I line  $\lambda 7511.02 \text{ \AA}$  deviate considerably in comparison with those for other high-excitation lines. For Fe II lines we used the *real* observations obtained by FK, which includes seven lines.

## 5.2. NLTE abundance correction

Our NLTE simulation reveals that Fe II lines in all the atmospheric models considered do not suffer in fact from NLTE effects. However, this is not the case for the Fe I lines. The LTE abundances derived from the Fe I lines are lower compared with NLTE values. Our computations clearly demonstrate that for the fixed value of metallicity the NLTE corrections are very sensitive to the changes in  $T_{\text{eff}}$  and  $\log g$ . The NLTE correction increases with  $T_{\text{eff}}$  due to the ultraviolet overionization effects. For the same  $T_{\text{eff}}$  a larger gravity results in larger NLTE abundance corrections. The mean  $\delta \log \epsilon$  are in the range 0.2 – 0.35 dex.

The NLTE abundance corrections for individual Fe I lines and for the stellar parameters of

BD + 23°3130 suggested by FK are plotted in Figure 5. The abundance corrections are largely independent on the excitation potential up to  $\chi \approx 2$  eV. However,  $\delta \log \epsilon$  decreases when the lines with  $\chi > 2$  eV are considered. The mean value of the NLTE abundance correction  $\delta \log \epsilon$  for the Fe I lines is 0.22 dex while for the Fe II lines there are no corrections for departures from LTE. Although the standard deviation of the abundance derived from Fe I lines is not very large (0.07 dex) there is a trend with  $\chi$  and a clear gap of 0.11 dex between the abundances derived from the “low” ( $\chi < 3.8$  eV) and “high” ( $\chi > 3.8$  eV) excitation lines. In general, the gap is smaller in the case of LTE. It is also interesting to point out that dependence on the line strength is less pronounced.

Our computations confirm the results by Thevenin & Idiart that the LTE Fe analysis in very metal-poor stars strongly underestimates gravities and metallicities. If we take into account the NLTE abundance corrections, the stellar parameters suggested by FK do not meet the condition requiring equal abundances derived from the Fe I and Fe II lines. The abundance difference due to neglect of the NLTE effects in the ionization equilibrium balance amounts to 0.2 dex. We found that the parameters used by Israelian et al. (1998) do not meet the conditions listed in 5.1.1 either. Figure 6 shows that a model similar to the one used by FK but with a gravity which is higher by 0.5 dex, is able to improve the situation considerably. With such model the difference in abundances derived from Fe I and Fe II lines becomes only 0.026 dex while the standard deviation from the mean abundance derived from the Fe I lines is 0.06. The gap between “low” ( $\chi < 3.8$  eV) and “high” ( $\chi > 3.8$  eV) excitation lines has also decreased to 0.07 dex.

### 5.3. Uncertainties in the NLTE analysis

Classical abundance determination depends on a large number of parameters. We evaluated the sensitivity of the abundances,  $\log \epsilon$ , derived from the Fe I and Fe II lines to the uncertainties of the most important parameters.

Several tests showed that a change in the enhancement factor,  $E$ , of the van der Waals damping constant,  $\gamma_6$ , from 1.5 to 2.0 produces changes of less than 0.04 dex in the Fe I abundance and can be neglected. The strongest low-excitation lines display the largest errors. The lines with equivalent widths  $EW < 80$  mÅ are insensitive to the uncertainties in  $E$ -factors. Fortunately, all Fe I and Fe II lines from Table 5 have equivalent widths smaller than this value.

The values of microturbulent velocity ( $V_t$ ) used by Israelian et al. (1998), and FK for BD+23°3130 differ in  $0.35 \text{ km s}^{-1}$ . Our tests show that Fe I lines with  $EW \approx 80$  mÅ and  $\chi < 3$  eV are most sensitive to  $V_t$ . However, even in that case the influence of the microturbulence uncertainties could be reduced or even eliminated by using lines with  $EW < 30$  mÅ. It turned out that the change in  $\log \epsilon$  corresponding to  $0.35 \text{ km s}^{-1}$  for the Fe I lines listed in Table 6 is  $\sim 0.04$  dex. Thus, the influence of uncertainties in the microturbulent velocity on the abundance derived from Fe I lines is negligibly small.

The accuracy of the oscillator strengths has a strong influence on the dispersion and the mean value of the iron abundance derived from Fe I and Fe II lines. In our study we used for low-excitation lines ( $\chi < 3$  eV) mainly the Oxford  $gf$  values (Blackwell et al. 1979a, 1979b, 1980, 1982a, 1982b, 1982c, 1984, 1986, 1995). The Oxford set does not contain any lines with  $\chi > 3$  eV. Our sample of the high-excitation lines is dominated by  $gf$  values measured by O’Brian et al. (1991) and the Kiel–Hannover group (Bard, Kock, & Kock 1991; Holweger et al. 1991, 1995). There is also a large set of the Fe I lines whose measured oscillator strengths are taken from the old sources (compilation by Fuhr et al. 1988).

Several authors (Grevesse & Noels 1993; Lambert et al. 1996; Grevesse & Sauval 1998) suggest that  $gf$  values of the higher-excitation Fe I lines that come from laboratory measurements provide likely less accurate results than those from the  $gf$  values of low-excitation lines. The use of the oscillator strengths mentioned above opened a new “iron problem” (Grevesse & Noels 1993) ‘namely the behavior of the abundance derived from Fe I lines vs. the excitation energy for a very large range of  $\chi$ , from 0 to 7.5 eV, observed in the solar spectrum’. The solar photospheric abundances found from the low-excitation lines using  $gf$  values of the Oxford group turns out to be systematically larger than those from high-excitation lines obtained with  $gf$  measured by Kiel–Hannover group and by O’Brian et al. (1991). Since  $gf$  values and abundance values enter the line extinction coefficient as a product, such behavior might be attributed to a  $gf$  systematic trend of about 0.06 dex (Bard et al. 1991; Holweger et al. 1995; Lambert et al. 1996). Another point of view is to attribute the trend to differences in the atmospheric properties of low- and high-excitation lines (Blackwell et al. 1995) or both effects together (Kostik, Shchukina, & Rutten 1996; Grevesse & Sauval 1998).

The most accurate Fe II oscillator strengths are not yet as accurate as for the Fe I lines. Following FK we used  $gf$  values obtained by Biémont et al. (1991) and Kroll & Kock (1987). A discussion of these and other sources of the oscillator strengths has been given recently by Grevesse & Sauval (1999) and Lambert et al. (1996). The mean uncertainty in the  $gf$  values for Fe II lines is found to be in the range  $\pm 0.05$ – $0.07$  dex, which corresponds to an abundance dispersion  $\sim 0.1$  dex. Uncertainties of the NLTE abundance corrections  $\delta \log \epsilon$  are discussed in detail by Shchukina & Trujillo Bueno (2000). The values  $\delta \log \epsilon$  are not very sensitive to uncertainties in collisional rates, photoionization cross-sections, continuum opacity, etc. The errors introduced by uncertainties in these parameters may lead to errors in the mean NLTE abundance,  $\delta \log \epsilon$ , of about  $\pm 0.03$  dex.

#### 5.4. Errors of the stellar parameter determinations

Summing up the analyses completed above, we conclude that the largest errors in the iron abundance determination using Fe I lines are expected to be caused by neglecting the NLTE effects. The largest errors in the abundance derived from Fe II lines are caused by the uncertainties in the oscillator strengths (if we exclude the errors in EW measurements). To what extent can

these errors influence the stellar parameters determination for the star BD + 23°3130?

Our computations show that the variations in  $T_{\text{eff}}$  primarily affect the abundance derived from Fe I lines but make little difference to the abundance from Fe II lines. Abundance changes for Fe I lines that result from a 270 K change in effective temperature are in the range  $\sim 0.26$  for LTE case and  $\sim 0.36$  dex for NLTE. In the case of Fe II lines they are an order of magnitude smaller. On the contrary, for Fe II lines the gravity dependence is much more pronounced, while for Fe I lines it is negligibly small. As a result, small errors in the Fe I abundances can only be compensated for by large changes in the assumed gravity. Or small errors in Fe II abundances can only be fixed by large changes in the assumed effective temperature. Our computations show that for the NLTE  $\delta \log \epsilon$  range 0.2–0.35 dex obtained using Fe I lines the correction in  $\log g$  may reach  $\sim 0.5$  dex in the cooler model ( $T_{\text{eff}} = 4850$  K) or even more in the hotter one ( $T_{\text{eff}} = 5130$  K). An abundance dispersion of 0.1 dex for Fe II lines causes dispersion of  $T_{\text{eff}}$  of 100 K. To reduce the latter effect it would be extremely desirable to enlarge the set of Fe II lines. It is obvious that the small seven-line sample can be a source of serious troubles in stellar parameter determinations.

### 5.5. The “best-choice” parameters of BD + 23°3130 and its oxygen abundance

Our computations are aimed at finding the NLTE solution that gives the minimum standard deviation,  $\sigma$ , of the mean abundance and satisfies the criteria discussed in Section 5.1.1. If we neglect the offset in abundances derived from the high-excitation ( $\chi > 3.8$  eV) and low-excitation ( $\chi < 3.8$  eV) lines, then the best model is the one displayed in Figure 6. The “best-choice” stellar parameters for this NLTE case turn out to be  $T_{\text{eff}} = 4825$  K,  $\log g = 2.5$ , and  $[\text{Fe}/\text{H}] = -2.66$ . The top panel shows the NLTE equivalent widths for the atmospheric model represented by these parameters against LTE values computed for the model with parameters by FK. Agreement between “quasi-observed” equivalent widths and those obtained in NLTE is quite satisfactory. However, if the Fe I line sample is divided into a “low” ( $\chi < 3.8$ ) eV and “high” ( $\chi > 3.8$ ) eV samples, the mean NLTE abundances are  $4.86 \pm 0.05$  and  $4.79 \pm 0.06$  for the “low” and “high” samples, respectively. This means that even this solution cannot be considered as *final* given the abundance offset found for the two samples of Fe lines.

We could not find a model which did not show an abundance gap between “low-” and “high-” excitation lines. This failure can be attributed to our poor knowledge of the atmospheric model structures and is possible due to some 3D and/or hydrodynamical effects.

This shortcoming can possibly be avoided if we concentrate our study only on the high-excitation lines with  $\chi > 3.8$  eV. This approach can be justified for the following reasons: a) the high-excitation lines are sensitive to NLTE effects in much less degree than low excitation ones and therefore to many uncertain factors such as overionization, granulation, geometry, etc.; b) the high-excitation lines are insensitive to the microturbulence; c) they are also insensitive to the damping factors; d) there probably exists a  $\log gf$  versus  $\chi$  trend for the low excitation lines;

and e) the high excitation lines are less affected by 3D and hydrodynamical effects (Shchukina & Trujillo Bueno 2000, Grevesse & Sauval , 1998, 1999).

Limiting our computations to 17 high-excitation lines, we are left with only one criterion for the selection of the “best model”. The only demand on the model parameters will be the minimum abundance scatter derived from the high-excitation Fe lines and the agreement between  $\log \epsilon(\text{Fe I})$  and  $\log \epsilon(\text{Fe II})$ . Results from four models are presented in Table 6. It is clear that the model with  $T_{\text{eff}} = 5130$  K and  $\log g = 3.0$  is the “best choice”. We can give more weight to this model since the gravity derived from the *Hipparcos* parallax is  $\log g = 3.05 \pm 0.25$ .

An important conclusion that follows from the NLTE analysis of Fe I lines is that the surface gravity of the star BD + 23°3130 derived using LTE approach is in error by at least  $\sim 0.5$  dex. In addition, the metallicity of the star has to be increased as well using the mean NLTE abundance correction,  $\delta \log \epsilon \approx 0.2$  dex.

#### 5.5.1. The oxygen abundance

FK did not detect the [O I] line at 6300 Å establishing an upper limit to its equivalent width of 1 mÅ. They argued that the parameters used by Israelian et al. (1998) would predict an [O I] absorption at 6300 Å with a larger EW which was not observed. However, given the S/N $\sim 250$  of their spectrum of BD +23°3130, one cannot claim a detection of absorption features with  $\text{EW} \leq 2$  mÅ, and errors in the EW for any barely detected line would have been at least 0.7 mÅ (although a more realistic value would be 2 mÅ), implying +0.2 and  $-0.5$  dex error in the [O/H] value (see Figure 4). Moreover, to this error we must add the systematic one due to uncertainties in gravity and effective temperature, which makes the total error in the oxygen abundance from the [O I] line very large. In conclusion, the failure to detect the forbidden line cannot be used to question the validity of the abundances derived from the OH lines and triplet. The new really high S/N measurement of the forbidden line in this star performed by Cayrel et al. (2000), using UVES at VLT, of  $\text{EW}=1.5\pm 0.3$  mÅ is perfectly consistent with our determinations of OH and triplet lines definitely solving the controversy. We show in what follows that there is consistency between the abundances inferred from the three oxygen indicators.

Assuming our stellar parameters, the EW measurement by Cayrel et al. (2000) for the forbidden line, our new triplet observations and the OH measurements by Israelian et al. (1998), we find  $[\text{O}/\text{H}]=-1.61\pm 0.15$ ,  $-1.5\pm 0.14$ ,  $-1.45\pm 0.33$ , respectively. There is a clear agreement between these three indicators given the error bars from each measurement. We interpret this as an indication that any 3D correction to the OH abundance, or NLTE correction for triplet abundance, is on the order of 0.15 dex. The agreement is even better (within 0.07 dex) if we employ models without convective overshooting. We conclude that in this cool subgiant it is possible to find a consistent determination of oxygen abundances using 1D models and stellar effective temperature from IRFM based calibration and gravity from *Hipparcos* parallax and/or

Fe NLTE analysis. The plot in figure 7 shows the difference in oxygen abundances derived for OH and [O I] in a number of stars whose parameters have been estimated in this way. These stars cover the metallicity range from  $-1$  to  $-2.5$  and strongly support the reliability of the linear trend in oxygen abundances as metallicity decreases. Four of these stars are listed in Table 4 of Israelian et al. (1998) and two others were studied by FK. The [O I] abundance ( $[O/H]=-1.52$ ) for the star BD+37°1458 ( $[Fe/H]=-2.1$ ) has been estimated from the equivalent width of the [O I] line using an *Hipparcos*-based gravity ( $\log g=3.35\pm 0.21$ ) and effective IRFM temperature  $T_{\text{eff}} = 5260 \pm 100$  K from Israelian et al. (1998). Using the same stellar parameters we find excellent agreement with the oxygen abundance  $[O/H]=-1.60$  derived from the OH lines observed by Israelian et al. (1998).

Using a different calibration, Carretta et al. (2000) have claimed that their oxygen NLTE analysis yields the same O abundances from both permitted and forbidden lines for stars with  $T_{\text{eff}} > 4600$  K. If this had been the case, there would have been no problems with oxygen abundance derived from the triplet and the forbidden line in BD +23°3130. Assuming the parameters of FK for this star, one can find from the triplet an LTE abundance  $[O/H] = -1.39$ . In this parameter range the NLTE abundance correction for the triplet is about  $-0.1$  according to Carretta et al. (2000) and Mishenina et al. (2000). Thus, the  $[O/H] = -1.39$  ratio obtained from the triplet is in odds with  $[O/H] = -2.49$  limit claimed from the undetected [O I] line by FK.

## 6. Discussion

### 6.1. A plateau versus linear trend

Our results support a linear increase of  $[O/Fe]$  with decreasing metallicity (Table 7 and Figures 8,9,10 and 11). This is in agreement with some previous analyses (Abia & Rebolo 1989, Tomkin et al. 1992, King & Boesgaard 1995, Cavallo et al. 1997, Israelian et al. 1998, Boesgaard et al. 1999a, Mishenina et al. 2000, Takeda et al. 2000) but at odds with others (Barbuy 1988, Kraft et al. 1992, Carretta et al. 2000); there appears to be a clear dichotomy among authors who support a plateau in  $[O/Fe]$  for stars with  $[Fe/H] < -1$  and those who do not. The situation is made even more confusing by the fact that there is an overlap both of objects and of O indicators used by authors arriving at different conclusions. The comparison we made with the results of FK and Carretta et al. (2000), suggest that the discrepancies are rooted in the atmospheric parameters adopted by different authors. Differences in the observational data, in the 1-D models and NLTE treatment of the O I triplet lines are second order effects. The set of atmospheric parameters chosen is always debatable, however we wish to point out that our choice provides gravities which are in agreement with *Hipparcos* parallaxes and achieve consistency among different O indicators, when available. We independently derived metallicities from our spectra and only in one case from EWs taken from the literature (for G271-162). We discard any significant change in the slope of the  $[O/Fe]$  versus  $[Fe/H]$  relation in the whole metallicity range from 0 to  $-3.1$ . The corresponding increase in Fig. 11 can be fitted using a straight line with a slope  $-0.33\pm 0.02$  (taking the error

bars into account).

The existence of a *plateau* with  $[O/Fe] \sim 0.4$  at  $[Fe/H] < -1$  in metal-poor giants could be questioned. The results of Takeda et al. (2000) show that metal-poor giants may have  $[O/Fe] > 0.6$  in the metallicity range  $[Fe/H] < -2$ . To some extent different conclusions on the existence of a plateau may be derived from the same data set. Tomkin et al. (1992) point out that “.. a linear least squares fit to the 10 field giants ( $-3 \leq [Fe/H] \leq -1.7$ ) in Fig. 8 of Sneden et al provides a slope of  $-0.33 \pm 0.10$  for  $[O/Fe]$  vs  $[Fe/H]$ ...”. It is interesting that this slope derived from the data of Sneden et al. (1991) is in excellent agreement with our value and the slopes found by Israelian et al. (1998) and Boesgaard et al. (1999a), who provide  $-0.31 \pm 0.11$  and  $-0.35 \pm 0.03$ , respectively. In spite of this, the results of Sneden et al. (1991) are usually quoted as evidence against the plateau probably because they obtained  $[O/Fe]$  ratios lower than 0.6.

So what is the  $[O/Fe]$  vs.  $[Fe/H]$  relation for giants ? We can think of two possibilities. There is a real scatter in the range  $0.3 < [O/Fe] < 1$  at  $[Fe/H] < -1$ , which could be explained by a weakening of the forbidden lines in some of the evolved giants due to the presence of circumstellar matter. Indeed, differences in the published EWs of the forbidden line for some giants may support this hypothesis (work in preparation). If this is the case, then one cannot display both giants and unevolved subdwarfs on the same  $[O/Fe]$  vs.  $[Fe/H]$  graph (e.g., Carretta et al. 2000). It is also possible that giants follow the linear trend just as unevolved subdwarfs, but previous investigators have failed to discover this for two main reasons; 1) they did not use sufficiently high S/N (e.g.,  $S/N > 400$ ) to investigate uncertainties involved in the determination of oxygen abundance from the forbidden line at  $6300 \text{ \AA}$  in the most metal-poor targets of their samples and 2) the stellar parameters of the most metal-poor giants were not correct because NLTE effects were not taken into account. However, we cannot exclude the possibility that the plateau derived from the  $[O I]$  in giants is correct. Work is in progress to study the stellar parameters of several giants with  $[Fe/H] < -2$  by performing a NLTE analysis of Fe lines and investigating its impact on the oxygen abundances derived from OH, forbidden, and triplet lines.

## 6.2. Oxygen nucleosynthesis in the early Galaxy

The new data in ultra-metal-poor unevolved stars confirm the previous findings for a progressive rise in oxygen overabundances as we go to  $[Fe/H] < -2.5$ . In particular, the high  $[O/Fe]$  ratio in G64-12 provides evidence for enhanced oxygen production in the first nucleosynthesis events in our Galaxy. Can these high  $[O/Fe]$  ratios in ultra-metal-poor stars be understood in terms of massive star nucleosynthesis models?

The first attempts to explain the linear trend were made by Abia, Canal, & Isern (1991), and more recently Goswami & Prantzos (2000) have suggested three possible scenarios to explain the observed linear trend of  $[O/Fe]$ . The first possibility, which has already been explored in the literature, considers the early evolution of Type Ia SNe, which started to contribute Fe to the

ISM already in the epoch when  $[\text{Fe}/\text{H}] \sim -3.0$ . Goswami & Prantzos (2000) remark that this model cannot be accepted, as it also predicts similar linear trends for other  $\alpha$  elements which are not observed. However, we would like to recall that the “traditional” trend of  $\alpha$  elements (i.e., a unique *plateau* at  $[\text{Fe}/\text{H}] < -1$ ) has been challenged recently by Idiart & Thévenin (2000) on the basis of NLTE computations of  $\alpha$  elements. In addition, the observations indicate (Francois 1987, 1988) that the  $[\text{S}/\text{Fe}]$  ratio increases from approximately 0 to 0.7 in the metallicity range  $-1.5 < [\text{Fe}/\text{H}] < 0$ . There is no *plateau* observed at  $[\text{Fe}/\text{H}] < -1$ , and the models fail to account for the observed  $[\text{S}/\text{Fe}]$  ratios (Goswami & Prantzos 2000). This is confirmed by recent observations of Takeda et al. (2000), who report  $[\text{S}/\text{Fe}] = 1.11$  in the metal-poor ( $[\text{Fe}/\text{H}] = -2.72$ ) giant HD 88609. As a second possibility, Goswami & Prantzos (2000) mention the metallicity-dependent oxygen yields proposed by Maeder (1992). Given that the stellar mass loss at very low metallicity is poorly understood, one can propose a model in which  $[\text{O}/\text{Fe}]$  increases below  $[\text{Fe}/\text{H}] \sim -1$ , while  $[\alpha/\text{Fe}]$  is constant. However, Goswami & Prantzos (2000) argue that even this model is not acceptable, as it predicts  $[\text{C}/\text{Fe}]$  and  $[\text{N}/\text{Fe}]$  ratios increasing with  $[\text{Fe}/\text{H}]$  (which are not observed). The third model proposed by Goswami & Prantzos (2000) considers the possibility of having metallicity-dependent Fe and  $\alpha$ -element yields at  $[\text{Fe}/\text{H}] < -1$ . This is possible if/when the supernova layers inside the carbon-exhausted core are well mixed during the explosion (to have  $[\alpha/\text{Fe}] \sim \text{const.}$ , in the ejecta for any  $[\text{Fe}/\text{H}]$ ). This last model requires that the oxygen, carbon, and helium layers will escape with the same yields, independent on the metallicity, as they are loosely bound. Note that these models did not take into account stellar rotation which plays a very important role in low-metallicity massive stars (Maeder & Maynet 2000). Strong observational support for matter mixing, which occurs in SN ejecta during or prior to explosion comes from the analysis of the low-mass X-ray binary system Nova Sco 1994 (Israelian et al. 1999). If the mass of the black hole in Nova Sco 1994 is more than  $\sim 4 M_{\odot}$  (which is just a lower limit given by observations), then it must have “eaten” all Fe-group elements plus the  $\alpha$  elements Ti, Ca, and S. Some amount of Mg and Si, together with almost all the O, may escape the collapse and therefore appear in the supernova ejecta captured by the secondary. However, observations show that all  $\alpha$  elements are uniformly enhanced in the atmosphere of the secondary star, and that therefore there must have been some mixing in the supernova ejecta. Most probably, this system is a relic of a hypernova that left a massive black hole and ejected similar amounts of  $\alpha$  elements (Israelian et al. 1999; Brown et al. 2000).

The yields from standard Type II supernovae have been investigated by a number of authors (e.g., Woosley & Weaver 1995; Thielemann, Nomoto, & Hashimoto 1996). It is well known that stellar yields are influenced by metallicity. Low mass-loss rates in very metal-poor massive stars lead to more massive He cores, and therefore more He is converted into oxygen (Maeder 1992). In contrast, the most massive solar-metallicity stars ( $M_{\text{ZAMS}} > 40 M_{\odot}$ ) go through a Wolf–Rayet phase where the mass loss is very efficient and end up with low-mass (4–6  $M_{\odot}$ ) He cores (Maeder & Meynet 1989). It is well known (Woosley 1996; Fryer, Woosley & Heger 2000) that during the contraction phase of helium cores with  $M \geq 40 M_{\odot}$  the temperature in the center of the star gets very high ( $\geq 3 \times 10^9 \text{K}$ ) while the density remains low. This favours the electron-positron

pair instability which leads to explosive oxygen or even silicon burning. It is interesting that the pair-creation supernovae produced by stars with  $M_{\text{ZAMS}} = 150\text{--}200M_{\odot}$  and  $Z = 0.0004$  lead to the formation of CO cores with  $M_{\text{CO}} = 60\text{--}100 M_{\odot}$ . A complete thermonuclear disruption of these objects produces very large amounts of oxygen and carbon (see Figure 2 in Portinari 2000). As a matter of fact, the maximum amount of oxygen at  $Z = 0.0004$  is produced not by  $20\text{--}25 M_{\odot}$  progenitors but by  $M_{\text{ZAMS}} = 150\text{--}200 M_{\odot}$  stars (Portinari 2000). Thus, it is possible that the early ISM of our Galaxy has been polluted by very massive CO cores of the first pair-creation supernovae. This idea is supported by Qian & Wasserburg (2000), who on the basis of three-component mixing model for the evolution of O relative to Fe, suggest a linear rise of [O/Fe] if the contribution of the first very massive stars is taken into account. The stability of ultra-metal-poor very massive stars was investigated recently by Baraffe, Heger & Woosley (2000) who concluded that such stars could take an active role in the nucleosynthesis of the early Galaxy.

Our observations suggest that the Fe production sites were active already in the early halo. Recently, Nomoto et al. (1999) have presented a model of an exploding CO core with a mass of  $12\text{--}15 M_{\odot}$ , and an explosion energy of  $2\text{--}5 \times 10^{52}$  erg in order to explain the observations of the hypernova SN1998bw. The progenitor of the CO core initially had  $M_{\text{ZAMS}} = 40 M_{\odot}$  and large angular momentum. Placing a mass cut-off at  $2.9 M_{\odot}$  Nomoto et al. (1999) have computed that  $0.7 M_{\odot}$  of  $^{56}\text{Ni}$  is ejected; the amount required to explain observations of SN1998bw. It is possible that the linear trend can be explained by an increasing role of hypernovae in the early epochs of the formation of the Galaxy (i.e.,  $[\text{Fe}/\text{H}] < -1$ ). The estimated Galactic rate of Type Ic hypernovae is  $10^{-3} \text{ yr}^{-1}$  (Hansen 1999) but it could have been much higher in the early Galaxy. Small mass-loss rates due to the low metallicity in the first generations of massive halo stars could have led to large helium cores and the conservation of the primordial angular momentum. Since hypernovae are favored by stars with a large helium core mass and rapid rotation, we anticipate significant sulfur (e.g. Takeda et al. 2000) and iron production in the early Galaxy following the yields computed by Nomoto et al. (1999). Whether the objects which started to produce large amounts of Fe in the very early halo were metal-poor progenitors of the first hypernovae, very massive stars, or other types of supernovae remains to be solved by future investigations.

Accelerated protons and  $\alpha$  particles in cosmic rays interact with ambient CNO in the ISM and create beryllium and boron. According to the standard Galactic cosmic ray (GCR) theory, these interactions in the general ISM should have given a quadratic relation between these elements and O that is not observed. Alternatively, spallation of cosmic ray CNO nuclei accelerated out of freshly processed material could account for the primary character of the observed early Galactic evolution of Be and B. Another production site is the collective acceleration by SN shocks of ejecta-enriched matter in the interiors of superbubbles. In these two cases, the evolution of Be should reflect the production of CNO from massive stars.

The dependence of  $\log(\text{Be}/\text{H})$  on  $[\text{Fe}/\text{H}]$  and on  $[\text{O}/\text{H}]$  is essentially linear but with different slopes:  $\sim 1.1$  and  $\sim 1.5$ , respectively, and similar behavior is found for boron (Molaro et al. 1997, García López et al. 1998; García López 1999; Boesgaard et al. 1999b, ). Three types of GCR

models exist at present that try to explain their observed evolution. These are 1) a pure primary GCR from superbubbles (Ramaty et al. 2000), 2) a hybrid model based on GCR and superbubble accelerated particles (Vangioni-Flam & Cassé 2000), which could be accomplished by a pure superbubble model (Parizot & Drury 2000), and 3) standard GCR (Olive 2000, Fields & Olive 1999). The models presented by Ramaty et al. (2000) and Olive (2000) show more consistency when a steady increase in  $[O/Fe]$  with decreasing metallicity is adopted. In addition, Ramaty et al. (2000) have proposed that a delay between the effective deposition times into the ISM of Fe and O (only a fraction of which condensed in oxide grains) can explain a linear trend in  $[O/Fe]$ . Their model also predicts a linear rise in  $[S/Fe]$ .

## 7. Conclusions

Oxygen abundances in several unevolved ultra-metal-poor stars have been derived using UV OH and O I IR triplet lines. It is found that the new abundances from both indicators confirm the linear trend of  $[O/Fe]$  vs.  $[Fe/H]$  first reported by Abia and Rebolo (1989) and more recently by Israelian et al. (1998) and Boesgaard et al. (1999a). In G64-12, the most metal-poor star in our sample, we find the highest  $[O/Fe]$  ratio at 1.17. Our best estimate of the slope in the trend  $[O/Fe]$  versus  $[Fe/H]$  is  $-0.33 \pm 0.02$ .

A detailed NLTE analysis of Fe I lines has been carried out for the subgiant star BD+23 3130 providing more reliable stellar parameters, in particular a surface gravity in good agreement with the value derived from its accurate *Hipparcos* parallax. Using these parameters and taking into account the uncertainties involved in deriving oxygen abundances from the weak forbidden line, we argue that the discrepancy noticed by FK can no longer be sustained. New measurements of the forbidden line by Cayrel et al. (2000) confirm our conclusions. There is no discrepancy between OH, triplet and forbidden line in BD+23 3130 when 1D ATLAS9 models are employed. Similar good agreement between the OH lines and the forbidden lines is found for several other metal-poor unevolved stars.

Examination of several scenarios for nucleosynthesis in low-metallicity Type II supernova and/or hypernovae provides a variety of possible explanations for the increase of oxygen overabundance with decreasing metallicity in the early Galaxy.

## 8. Acknowledgments

The data presented here were obtained with the William Herschel Telescope, operated on the island of La Palma by the Isaac Newton Group in the Spanish Observatorio del Roque de los Muchachos of the Instituto de Astrofísica de Canarias, the public data released from the UVES commissioning and Science Verification at the VLT Kueyen telescope, European Southern Observatory, Paranal, Chile, as well as with the W. M. Keck Observatory, which is operated as a

scientific partnership among the California Institute of Technology, the University of California, and the National Aeronautics and Space Administration. The Observatory was made possible by the generous financial support of the W. M. Keck foundation. We are grateful to Ya. V. Pavlenko for providing the code WITA3 and for helpful discussions. N. S. would like to thank R. Kostik for several useful discussions. We thank Carlos Allende Prieto for many discussions about *Hipparcos* gravities of the program stars and for providing us the gravity values for BD +23°3130 and BD +37°1458 . Ilia Ilyin is thanked for helping with the reduction of NOT/SOFIN spectra. This research was partially supported by the Spanish DGES under projects PB95-1132-C02-01 and PB98-0531-C02-02 and also by a NATO grant 950875.

## REFERENCES

- Abia, C., & Rebolo, R. 1989, ApJ, 347, 186
- Abia, C., Canal, R. & Isern, J. 1991, ApJ, 366, 198
- Allende Prieto, C., García López, R. J., Lambert, D. L., & Gustafsson, B. 1999, ApJ, **527**, 879
- Allende Prieto, C. & Lambert, D. L. 2000, AJ, 119, 2445
- Alonso, A., Arribas, S., & Martínez-Roger, C. 1996, A&A, 313, 873
- Anders, E. & Grevesse, N. 1989, Geochim. Cosmochim. Acta, 53, 197
- Asplund, M., Nordlund, A., Trampedach, R. & Stein, R. 1999, A&A, 346, L17
- Asplund, M. 2000, in "Oxygen Abundances in Old Stars and Implications to nucleosynthesis and cosmology", IAU 24 General Assembly, Barbuy, B. (eds.), in press
- Auer, L. H., Fabiani Bendicho, P. & Trujillo Bueno, J. 1994, A&A, 292, 599
- Balachandran, S. & Bell, G. 1998, Nature, 392, 791
- Baraffe, I. Heger, A. & Woosely, S., 2000, ApJ, submitted
- Barbuy, B. 1988, A&A, 191, 121
- Bard, A., Kock, A. & Kock, M. 1991, A&A, 248, 315
- Belyaev, A. K., Grosser, J., Hahne, J. & Menzel, T. 1999, Phys. Rev. A, 60, 2150
- Bessell, M. S., Sutherland, R. S., & Ruan, K. 1991, ApJ, 383, L71
- Biémont, E., Baudoux, M., Kurucz, R., Ansbacher, W. & Pinnington, E. 1991, A&A, 249, 539
- Blackwell, D., Booth, A., Haddock, D., Petford, A. & Leggett, S. 1986, MNRAS, 220, 549

- Blackwell, D., Booth, A. & Petford, A. 1984, A&A, 132, 236
- Blackwell, D., Lynas-Gray, A. & Smith, G. 1995, A&A, 296, 217
- Blackwell, D., Petford, A., Shallis, M. & Simmons, G. 1982a, MNRAS, 199, 43
- Blackwell, D. E., Ibbetson, P., Petford, A. D. & Shallis, M. J. 1979a, MNRAS, 186, 633
- Blackwell, D. E., Petford, A. D. & Shallis, M. J. 1979b, MNRAS, 186, 657
- Blackwell, D. E., Petford, A. D., Shallis, M. J. & Simmons, G. J. 1980, MNRAS, 191, 445
- Blackwell, D. E., Petford, A. D. & Simmons, G. J. 1982b, MNRAS, 201, 595
- Blackwell, D. E., Shallis, M. J. & Simmons, G. J. 1982c, MNRAS, 199, 33
- Boesgaard, A.M., King, J.R., Deliyannis, C. P., & Vogt, S.S. 1999a, AJ, 117, 492
- Boesgaard, A.M., Deliyannis, C. P., King, J.R., Ryan, S.G., & Vogt, S.S. & Beers, T. 1999b, AJ, 117, 1549
- Brown, G. E., Wijers, R. A. M. J., Lee, C.-H., Lee, H.-K., Israelian, G. & Bethe, H. A. 2000, New Astronomy, 5, 191
- Carney, B. W. 1983, AJ, 88, 623
- Carretta, E., Gratton, R. & Sneden, C. 2000, A&A, 356, 238
- Castelli F., Gratton R.G., Kurucz R.L., 1997, A&A, 318, 841
- Cavallo, R. M., Pilachowski, C. A., & Rebolo, R. 1997, PASP, 109, 226
- Cayrel, R. 1988, in *"The impact of Very High S/N Spectroscopy on Stellar Physics"*, Cayrel de Strobel, G. & Spite, M. (eds.), Dordrecht, Kluwer, 345
- Cayrel, R., et al., 2000, in *"Oxygen Abundances in Old Stars and Implications to nucleosynthesis and cosmology"*, IAU 24 General Assembly, Barbuy, B. (eds.), in press
- Edvardsson, B., Andersen, J., Gustafsson, B., Lambert, D. L., Nissen, P. E., & Tomkin, J. 1993, A&A, 275, 101
- Fields, B.D., & Olive, K.A. 1999, ApJ, 516, 797
- Fleck, I., Grosser, J., Schnecke, A., Steen, W. & Voigt, H. 1991, JPhB 24, 4017
- Francois, P. 1987, A&A, 176, 294
- Francois, P. 1988, A&A, 195, 226
- Fryer, C., Woosley, S. & Heger, A. 2000, ApJ, submitted

- Fuhr, J. R., Martin, G. A. & Wiese, W. L. 1988, *J. Phys. Chem. Ref. Data*, 17, suppl. 4
- Fullbright, J. & Kraft, R. 1999, *AJ*, 118, 527
- García López, R. J. 1999, in *LiBeB, Cosmic Rays, and Related X- and Gamma-Rays*, Eds. R. Ramaty, E. Vangioni-Flam, M. Cassé, & K. Olive, *ASP Conf. Series*, 171, p. 77
- García López, R. J., Lambert, D. L., Edvardsson, B., Gustafsson, B., Kiselman, D., & Rebolo, R. 1998, *ApJ* 500, 241
- Gigas, D. 1986, *A&A*, 165, 170
- Gillis, J. R., Goldman, A., Stark, G., & Rinsland, P. 2000, *J. Quant. Spec. Radiat. Transf.*, in press
- Goldman, A., & Gillis, J. R. 1981, *J. Quant. Spec. Radiat. Transf.*, 25, 111
- Goswami, A. & Prantzos, N. 2000, *A&A*, in press
- Gratton, R., Carretta, E. & Castelli, E. 1996, *A&A*, 314, 191
- Grevesse, N. & Noels, A. 1993, *Physica Scripta*, T47, 133
- Grevesse, N. & Sauval, A. 1998, *Space Science Reviews*, 85, 161
- Grevesse, N. & Sauval, A. 1999, *A&A*, 347, 348
- Hansen, B.M.S. 1999, *ApJ*, 512, L117
- Holweger, H., Bard, A., Kock, A., Kock, M. 1991, *A&A*, 241, 545
- Holweger, H., Heise, C. & Kock, M. 1990, *A&A*, 232, 510
- Holweger, H., Kock, M. & Bard, A. 1995, *A&A*, 296, 233
- Idiart, T. & Thevenin, F. 2000, *astro-ph/0004337*
- Israelian, G., García López, R. J. & Rebolo, R. 1998, *ApJ*, 507, 805
- Israelian, G., Rebolo, R., Basri, G., Casares, J., & Martin, E. L. 1999, *Nature*, 401, 142
- King, J. R., & Boesgaard, A. M. 1995, *AJ*, 109, 383
- Kiselman, D. 1993, *A&A*, 275, 269
- Kostik, R. I., Shchukina, N. G. & Rutten, R. J. 1996, *A&A*, 305, 325
- Kraft, R. P., Sneden, C., Langer, G. E., & Prosser, C.F. 1992, *AJ*, 104, 645
- Kroll, S. & Kock, M. 1987, *A&AS*, 67, 225

- Kurucz, R. L. 1992, private communication
- Lambert, D. L. 1978, MNRAS, 183, 249
- Lambert, D., Heath, J. E., Lemke, M. & Drake, J. 1996, Ap&SS, 103, 183
- Langer, G. E. 1991, PASP, 103, 177
- Maeder, A. 1992, A&A, 264, 105
- Maeder, A. & Meynet, G. 1987, A&A, 182, 243
- Maeder, A. & Meynet, G. 2000, ARA&A, in press
- Magain, P. 1988, in M. S. de G. C. Stobel (ed.), The Impact of High S/N Spectroscopy on Stellar Physics, Proceedings, Kluwer, Dordrecht, 485
- Magain, P., Zgao, G. 1996, A&A, 305, 245
- Mishenina, T., Korotin, S., Klochkova, V., & Panchuk, V. 2000, A&A, 353, 978
- Molaro P., Bonifacio P., Primas, F., 1995, Mem. S.A.It. 66, 323
- Molaro P., Bonifacio P., Castelli, F., Pasquini, L. 1997, A&A, 319, 593
- Nave, G, Johansson, S., Learner, R. C. M., Thorne, A. P. & Brawlt, J. W. 1994, ApJS, 94, 221
- Nissen, P. E., Gustafsson, B., Edvardsson, B., & Gilmore, G. 1994, A&A, 285, 440
- Nissen, P. E., Asplund, M., Hill, V. & D’Odorico, S. 2000, A&A, 357, L49
- Nomoto, K., Nakamura, T., Iwamoto, K., Umeda, H., and Mazzali, A. 1999, in *”Nuclei In Cosmos V”*, Prantzos, N. and Harissopulus, S. (eds.) Editions Frontieres, Paris, p. 252
- Norris, J. E., Ryan, S. G., Beers, T. C. 1997, ApJ, 488, 350
- O’Brian, T., Wickliffe, M., Lawler, J., Whaling, W., Brault, J. 1991, J. Opt. Soc. Am., B8, 1185
- Olive, K. 2000, in in L. da Silva, M. Spite, and J.R. de Medeiros (eds.), The Light Elements and their Evolution, IAU Symposium 198, in press
- Parizot, E. & Drury, L. 2000, A&A, 356, 66
- Pavlenko, Ya. V. 1991, Soviet Astr., 35, 212
- Perryman et al. 1997, The Main Hipparcos Catalogue, ESA
- Portinari, L. 2000, in A. Weiss, T. Abel and V. Hill (eds.), The First Stars, ESO Astrophysics Symposia, Springer, p. 137

- Qian, Y.-Z. & Wasserburg, G. J. 2000, ApJ, in press
- Ramaty, R., Scully, S., Lingenfelter, R. & Kozlovsky, B. 2000, ApJ, 534, 747
- Ruland, F., Holweger, H., Griffin, R., Griffin, R., Biehl, D. 1980, A&A, 92, 70
- Rutten, R. J. 1988, in R. Viotti, A. Vittone, M. Friedjung (eds.), Physics of Formation of FeII Lines Outside LTE, IAU Colloquium 94, Reidel, Dordrecht, p. 185
- Ryan, S. G., Norris, J. E., Beers, T. C. 1999, ApJ, 523, 654
- Shchukina, N., Trujillo Bueno, J. 1998, Kinematika i Fizika Nebesnich Tel, 14, 315
- Shchukina, N., Trujillo Bueno, J. 2000, ApJ, in press
- Snedden, C. 1973, ApJ, 184, 839
- Snedden, C., Kraft, R. P., Prosser, C.F., & Langer, G. E. 1991, AJ, 102, 2001
- Takeda, Y. 1995, PASJ, 47, 463
- Takeda, Y., Takeda-Hidai, M., Sato, S., Sargent, W.L., Lu, L., Barlow, T., Jugaku, J. 2000, ApJ, submitted
- Theilemann, F.-K., Nomoto, K., & Hashimoto, M. 1996, ApJ, 460, 108
- Thevenin, F. & Idiart, T. 1999, ApJ, 521, 753
- Thorburn, J. A. 1994, ApJ, 421, 318
- Tomkin, J., Lemke, M., Lambert, D. L., & Sneden, C. 1992, AJ, 104, 1568
- Trujillo Bueno, J. & Fabiani Bendicho, P. 1995, ApJ, 455, 646
- Vangioni-Flam, E. & Cassé, M. 2000, in L. da Silva, M. Spite, and J.R. de Medeiros (eds.), The Light Elements and their Evolution, IAU Symposium 198, in press
- Westin, J., Sneden, C., Gustafsson, B. & Cowan, J. 2000, ApJ, 530, 783
- Woosley, S. 1996, in Saas-Fee Advanced Course 15, *Nucleosynthesis and Chemical Evolution*, Geneva Observatory, Sauverny-Versoix
- Woosley, S. E., & Weaver, T. A. 1995, ApJS, 101, 181
- Zhao, G. & Magain, P. 1990, A&ASuppl., 86, 85

Table 1. Observing log.

Configuration	$\lambda/\Delta\lambda$	Spectral region (in Å)	Date	Target	$V$	Exp. time (s)	S/N
WHT/UES	30 000	5280–10300	1999 Jul 26	G64-37	11.13	6000	150
WHT/UES	30 000	5280–10300	1999 Jul 27	G268-32	12.11	7500	150
WHT/UES	50 000	4120–8100	1997 Jun 15	G64-37	11.13	3600	60
WHT/UES	50 000	4930–7940	1996 Oct 25	BD +23°3130	8.95	3600	250
WHT/UES	50 000	4930–7940	1996 Oct 25	G4-37	11.42	13 600	180
WHT/UES	50 000	4930–7940	1996 Oct 25	BD +03°740	9.81	3600	220
NOT/SOFIN	30 000	3800–10600	1999 May 31	BD +23°3130	8.95	2400	50
NOT/SOFIN	30 000	3800–10600	1998 Oct 06	LP 831-70	11.62	6600	80
NOT/SOFIN	30 000	3800–10600	1998 Oct 07	G268-32	12.11	4800	60
KeckI/HIRES	60 000	6430–8750	1999 Dec 4	G275-4	12.12	3600	170
KeckI/HIRES	60 000	6430–8750	1999 Dec 4	LP 831-70	11.62	2400	160
KeckI/HIRES	60 000	6430–8750	1999 Dec 4	G268-32	12.11	3600	170
KeckI/HIRES	60 000	6430–8750	1998 Jun 24	G275-4	12.12	1200	100
VLT/UVES	110 000	6052–8205	1999 Oct 11,12,13	G271-162	10.35	10800	300
VLT/UVES	40 000	3025–3918	1999 Oct 8,16	LP815-43	10.91	10800	100
VLT/UVES	40 000	3025–3918	1999 Oct 9	G275-4	12.12	9000	80
VLT/UVES	55 000	6652–10433	2000 Feb 15	G64-12	11.47	9600	100
VLT/UVES	55 000	3025–3918	2000 Feb 13,15	G64-12	11.47	20400	120

<sup>a</sup>The signal-to-noise ratio (S/N) is provided at 7760 and 3130 Å in the red and blue spectra, respectively.

Table 2. Parameters from the literature and this work

Star	$T_{\text{eff}}$	$\log g$	[Fe/H]	Ref.
G4-37	6050		−2.7	2
	6124		−2.78	3
	5837	4.23	−2.89	5
G64-12	6380	4.39	−3.12	1
	6220		−3.24	2
	6197		−3.52	3
	6318	4.2	−3.37	5
G64-37	6240		−3.15	2
	6376		−2.70	3
	6310	4.2	−3.22	5
G268-32	5841		−3.5	3
	6000	3.8	−2.7	4
	6090	3.86	−2.81	5
G271-162	5860	3.71	−2.05	1
	6135		−2.69	3
	6050	4.0	−2.46	5
G275-4	6000	4.39	−3.12	1
	6070		−3.24	2
	6168		−3.70	3
	6212	4.13	−3.32	5
LP 815-43	6380	4.39	−2.64	1
	6340		−3.00	2
	6423		−3.20	3
	6265	4.54	−3.05	5
LP 831-70	6000	4.40	−2.85	1
	6050		−3.32	2
	6119		−3.40	3
	6205	4.3	−2.97	5
BD +03°740	6146	3.98	−2.5	1
	6240		−2.7	2
	6401		−2.77	3
	6135	4.0	−2.93	5

References. — (1): Thevenin & Idiart 1999, (2): Ryan et al. (1999), (3): Thorburn 1994, (4): Norris et al. 1997, (5): present work.

Table 3. Abundances derived from the oxygen triplet and iron lines

Ion	$\lambda$ (Å)	$\log gf$	$\chi$	G4-37	G64-37	G268-32	G271-162	LP 831-70	BD +23°3130	BD +03°740	
O I	7771.95	0.358	9.14	7.41	<6.97	7.35	7.27	<7.08	7.50	7.07	
O I	7774.18	0.212	9.14	7.43		7.21	7.31		7.48	7.01	
O I	7775.40	-0.01	9.14	7.57		7.23	7.28		7.45		
Fe I	4271.774	-0.173	1.49		4.24	4.61	5.24	4.55	5.26		
Fe I	4325.775	0.006	1.61		4.21	4.73		4.45	5.23		
Fe I	4383.557	0.208	1.48		4.23	4.79		4.45	5.27		
Fe I	4415.135	-0.621	1.61		4.38	4.69	5.18	4.56	4.87		
Fe I	5227.192	-1.227	1.56	4.61	4.26	4.73		4.49	5.10	4.59	
Fe I	5232.952	-0.057	2.94	4.63	4.31	4.59	4.98		4.83	4.44	
Fe I	5269.550	-1.333	0.86	4.62	4.31	4.67		4.66	4.98	4.62	
Fe I	5397.141	-1.982	0.91	4.58	4.31	4.76	5.07	4.62	5.08	4.59	
Fe I	5405.785	-1.852	0.99	4.61	4.35	4.77	5.01	4.62	5.06	4.58	
Fe I	5429.706	-1.881	0.96	4.65	4.39	4.66			5.08	4.61	
Fe I	5434.534	-2.126	1.01	4.61	4.35	4.80	5.02		5.09	4.57	
Fe I	5569.630	-1.881	3.42	4.77			4.90			4.68	
O(mean)				7.47±0.09		7.26±0.07		7.29±0.03		7.48±0.03	7.04±0.04
Fe(mean)				4.63±0.06	4.30±0.06	4.71±0.07	5.06±0.12	4.55±0.08	5.07±0.14	4.59±0.07	

Table 4. Abundances derived from the OH and Fe I lines.

Ion	$\lambda$ (Å)	$\log gf_{\text{th}}$	$\log gf_{\text{ad}}$	$\chi$	G275-4	G64-12	LP815-43
OH	3085.199	-1.971	-2.060	0.843	6.70	7.15	6.90
OH	3123.948	-2.003	-2.086	0.204	6.90	7.05	6.80
OH	3127.687	-1.588	-1.590	0.612	6.85	6.95	6.70
OH	3128.286	-2.074	-2.070	0.209	6.90	7.10	6.85
OH	3139.169	-1.563	-1.762	0.760		6.95	
OH	3140.730	-1.994	-2.090	0.300		6.95	6.90
OH	3167.169	-1.544	-1.694	1.108		7.05	6.85
OH	3186.084	-1.859	-2.097	0.685	6.90	7.10	6.80
Fe I	3786.682	-2.185		1.01	4.26	4.23	4.43
Fe I	3787.891	-0.838		1.01	4.08	4.09	4.49
Fe I	3790.098	-1.739		0.99	4.23	4.21	4.53
Fe I	3820.436	0.157		0.86	4.15	4.07	4.46
Fe I	3821.187	0.198		3.27		4.20	4.52
Fe I	3825.891	-0.024		0.91	4.29	4.10	4.46
OH(mean)					6.85±0.09	7.05±0.08	6.82±0.09
Fe(mean)					4.20±0.08	4.15±0.07	4.48±0.04

<sup>a</sup>The line  $\lambda$  3140.73 Å has been added from the list of Nissen et al. (1994) and was also used by Boesgaard et al. (1999).

<sup>b</sup>The  $\log gf_{\text{th}}$ -values for the OH and Fe I lines are from Gillis et al. (2000) and O’Brian et al. (1991), respectively.  $\log gf_{\text{ad}}$  come from Israelian et al. (1998).

Table 5. Fe I line list for BD +23°3130

Wavelength	$\chi$	$\log gf$	Ref.	Mult. no.	Wavelength	$\chi$	$\log gf$	Ref.	Mult. no.
4011.710	2.450	-2.693	4	153	5415.200	4.386	0.504	4	1165
4055.030	2.559	-0.815	4	218	5424.070	4.320	0.576	4	1146
4076.630	3.211	-0.356	4	558	5476.571	4.103	-0.842	4	1062
4084.498	3.332	-0.597	4	698	5487.746	4.320	-0.650	5	1143
4085.300	3.241	-0.708	4	559	5525.552	4.191	-1.080	3	1062
4100.740	0.859	-3.179	1	18	5554.890	4.549	-0.444	4	1183
4112.960	4.178	-0.325	4	1103	5576.097	3.430	-1.000	4	686
4126.180	3.332	-0.959	4	695	5586.763	3.370	-0.100	3	686
4181.750	2.832	-0.187	4	354	5615.652	3.332	-0.188	7	686
4199.090	3.047	0.250	4	522	5662.525	4.178	-0.879	4	1087
4216.186	0.000	-3.356	1	3	5701.550	2.560	-2.220	1	209
4219.360	3.573	0.120	4	800	5934.660	3.929	-1.155	4	982
4224.170	3.368	-0.400	4	689	5956.700	0.860	-4.605	1	14
4276.680	3.882	-1.207	4	976	6003.030	3.882	-1.121	4	959
4282.400	2.176	-0.810	4	71	6065.480	2.610	-1.530	1	207
4285.440	3.237	-1.190	4	597	6136.610	2.450	-1.400	1	169
4326.750	2.949	-1.920	4	413	6136.900	2.200	-2.950	1	62
4388.410	3.603	-0.580	4	830	6151.620	2.180	-3.300	1	62
4439.880	2.279	-3.002	4	116	6173.340	2.220	-2.880	1	62
4445.470	0.087	-5.440	1	2	6200.320	2.610	-2.440	1	207
4484.227	3.603	-0.724	4	828	6219.280	2.200	-2.430	1	62
4528.610	2.176	-0.822	4	68	6230.730	2.560	-1.280	1	207
4581.510	3.241	-1.833	4	555	6240.660	2.220	-3.230	3	64
4602.944	1.485	-2.155	4	39	6246.334	3.600	-0.870	2	816
4647.430	2.949	-1.350	4	409	6252.550	2.400	-1.690	1	169
4733.596	1.490	-2.987	1	38	6265.130	2.180	-2.550	1	62
4736.780	3.211	-0.752	2	554	6280.630	0.860	-4.390	1	13
4957.603	2.808	0.043	4	318	6297.800	2.220	-2.740	1	62
4966.096	3.332	-0.879	2	687	6301.515	3.650	-0.720	3	816
4973.100	3.960	-0.955	4	984	6302.507	3.690	-1.150	6	816
4978.600	3.984	-0.940	4	966	6322.690	2.590	-2.430	1	207
5001.860	3.882	-0.004	4	965	6336.840	3.690	-0.860	3	816
5012.071	0.860	-2.642	1	16	6358.690	0.859	-4.468	1	13

Table 5—Continued

Wavelength	$\chi$	$\log gf$	Ref.	Mult. no.	Wavelength	$\chi$	$\log gf$	Ref.	Mult. no.
5044.210	2.850	-2.017	2	318	6393.600	2.430	-1.430	3	168
5049.825	2.280	-1.355	2	114	6400.010	3.600	-0.290	3	816
5162.270	4.178	0.019	2	1089	6411.658	3.650	-0.717	2	816
5166.286	0.000	-4.195	1	1	6421.355	2.280	-2.027	1	111
5171.600	1.485	-1.790	4	36	6430.851	2.180	-2.010	1	62
5198.710	2.220	-2.135	1	66	6481.880	2.280	-2.980	1	109
5202.339	2.180	-1.839	1	66	6494.980	2.390	-1.270	1	168
5217.389	3.210	-1.162	2	553	6593.880	2.430	-2.420	1	168
5232.946	2.940	-0.057	2	383	6609.120	2.560	-2.690	1	206
5242.495	3.630	-0.967	2	843	6677.993	2.692	-1.418	2	268
5247.052	0.087	-4.950	1	1	6750.150	2.420	-2.620	1	111
5250.212	0.120	-4.940	1	1	6945.200	2.420	-2.480	1	111
5253.460	3.280	-1.570	3	553	6978.850	2.480	-2.500	1	111
5322.040	2.280	-3.022	4	112	7511.045	4.178	0.099	2	1077
5324.185	3.210	-0.100	3	553	7748.281	2.949	-1.754	4	402
5393.174	3.240	-0.720	3	553	7945.878	4.386	0.094	4	1154

References. — (1): Blackwell et al. 1979a, 1979b, 1980, 1982a, 1982b, 1982c, 1984, 1986, 1995; (2): O’Brian et al. 1991; (3): Bard et al. 1991, Holweger et al. 1991, 1995; (4) Fuhr et al. 1988.

Table 6. Abundances derived from Fe I and Fe II lines in four different models for BD +23°3130

Abundance/model	4850/2.0	4825/2.5	4980/2.7	5130/3.0
$\log \epsilon$ (Fe I)	4.910±0.07	4.860±0.059	5.002±0.070	5.256±0.108
$\log \epsilon$ (Fe I) ( $\chi < 3.8\text{eV}$ )	4.930±0.057	4.860±0.050	5.024±0.053	5.290±0.084
$\log \epsilon$ (Fe I) ( $\chi > 3.8\text{eV}$ )	4.820±0.063	4.787±0.058	4.900±0.051	5.091±0.047
$\log \epsilon$ (Fe II)	4.717±0.121	4.886±0.122	4.972±0.122	5.089±0.116

Table 7. Stellar parameters and oxygen abundances in the sample of metal-poor unevolved stars

Star	$V - K$	$T_{\text{eff}}$	$\log g$	[Fe/H]	[Fe/H]	[O/H] <sub>Triplet</sub>	[O/H] <sub>OH</sub>	[O/Fe] <sub>Triplet</sub>	[O/Fe] <sub>Triplet</sub>	[O/Fe] <sub>OH</sub>	[O/Fe] <sub>OH</sub>
				LTE	NLTE*			LTE	NLTE*	LTE	NLTE*
G4-37	1.450	5837±80	4.23±0.3	-2.89±0.1	-2.59	-1.51±0.16		1.38	1.08		
G64-12	1.196	6318±150	4.20±0.3	-3.37±0.16	-3.05	-2.14	-1.88±0.31	1.23	0.91	1.49	1.17
G64-37	1.191	6310±110	4.20±0.3	-3.22±0.12	-2.90	< -2.01		<1.21	<0.89		
G268-32	1.306	6090±100	3.86±0.4	-2.81±0.12	-2.51	-1.72±0.18		1.09	0.79		
G271-162	1.320	6050±70	4.03±0.3	-2.46±0.14	-2.18	-1.69±0.16		0.77	0.5		
G275-4	1.254	6212±150	4.13±0.3	-3.32±0.17	-2.99	< -1.96	-2.08±0.32	<1.36	<1.03	1.24	0.91
LP 815-43	1.218	6265±125	4.54±0.3	-3.05±0.13	-2.74		-2.11±0.27			0.94	0.63
LP 831-70	1.251	6205±120	4.30±0.3	-2.97±0.14	-2.66	< -1.90		<1.07	<0.76		
BD +23°3130	1.97	5130±150	3.05±0.25	-	-2.43	-1.50±0.14	-1.45±0.33		0.93		0.98
BD +03°740	1.284	6135±100	4.00±0.1	-2.93±0.12	-2.63	-1.94±0.13		0.99	0.69		

NLTE\* refers to the [Fe/H] ratio estimated after Thévenin & Idiart (1999). See section 3 for details. The NLTE Fe abundance of BD + 23°3130 is estimated in this paper.

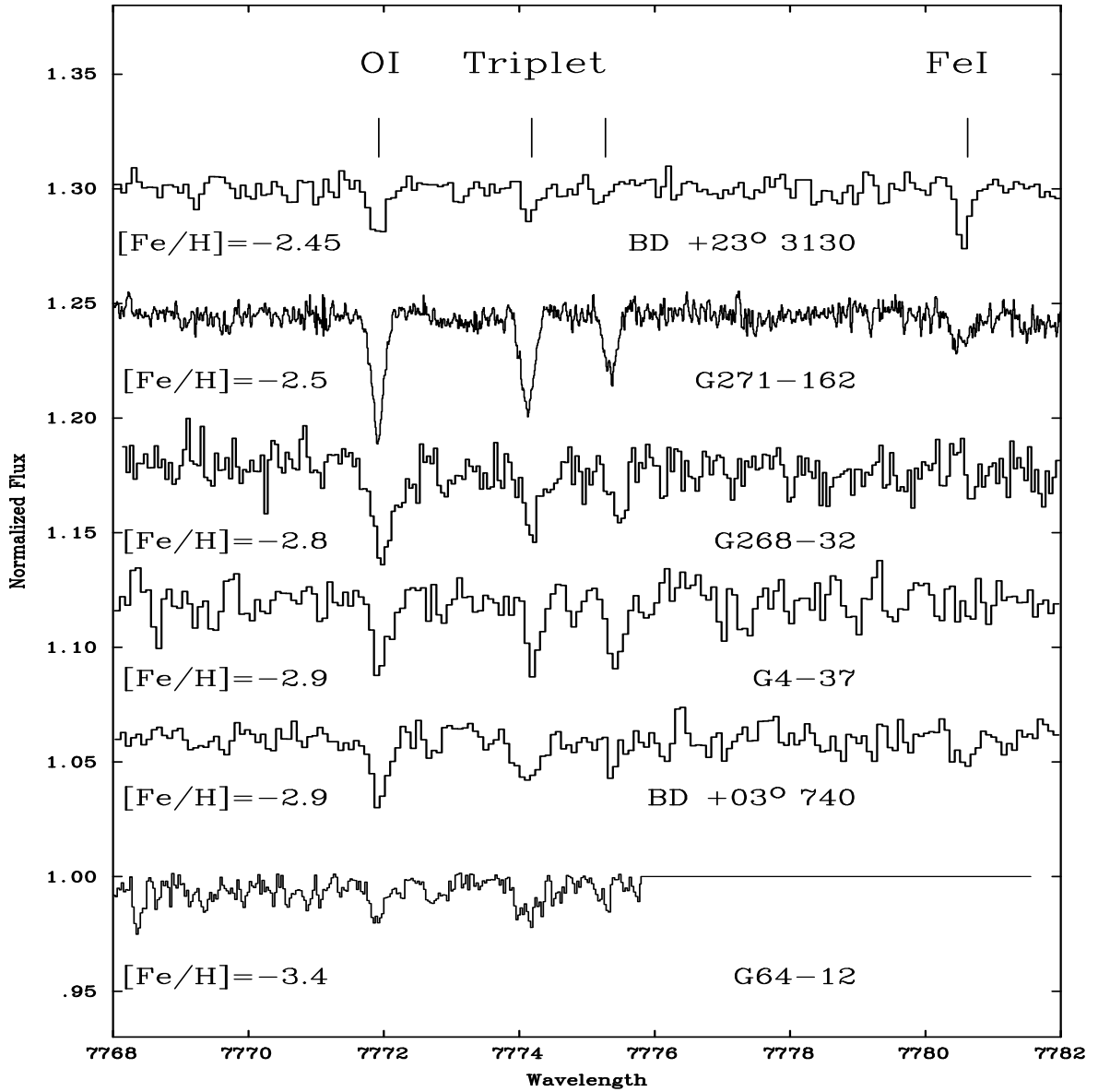


Fig. 1.— Oxygen triplet observed in the metal-poor subdwarfs. The metallicities quoted have been estimated in LTE.

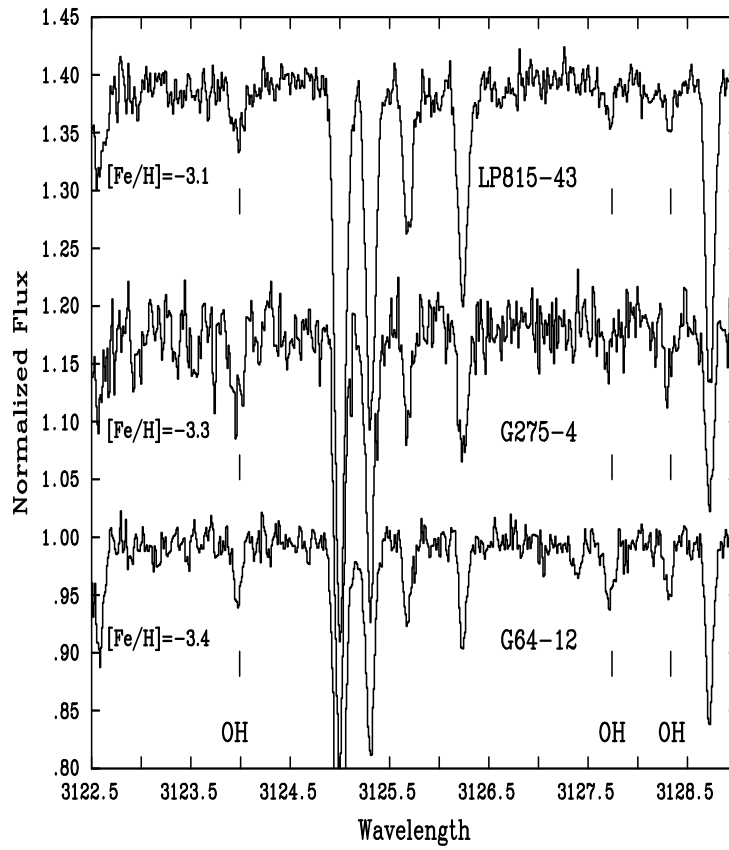


Fig. 2.— OH lines in the UVES spectra of three ultra-metal-poor subdwarfs. The metallicities quoted have been estimated in LTE.

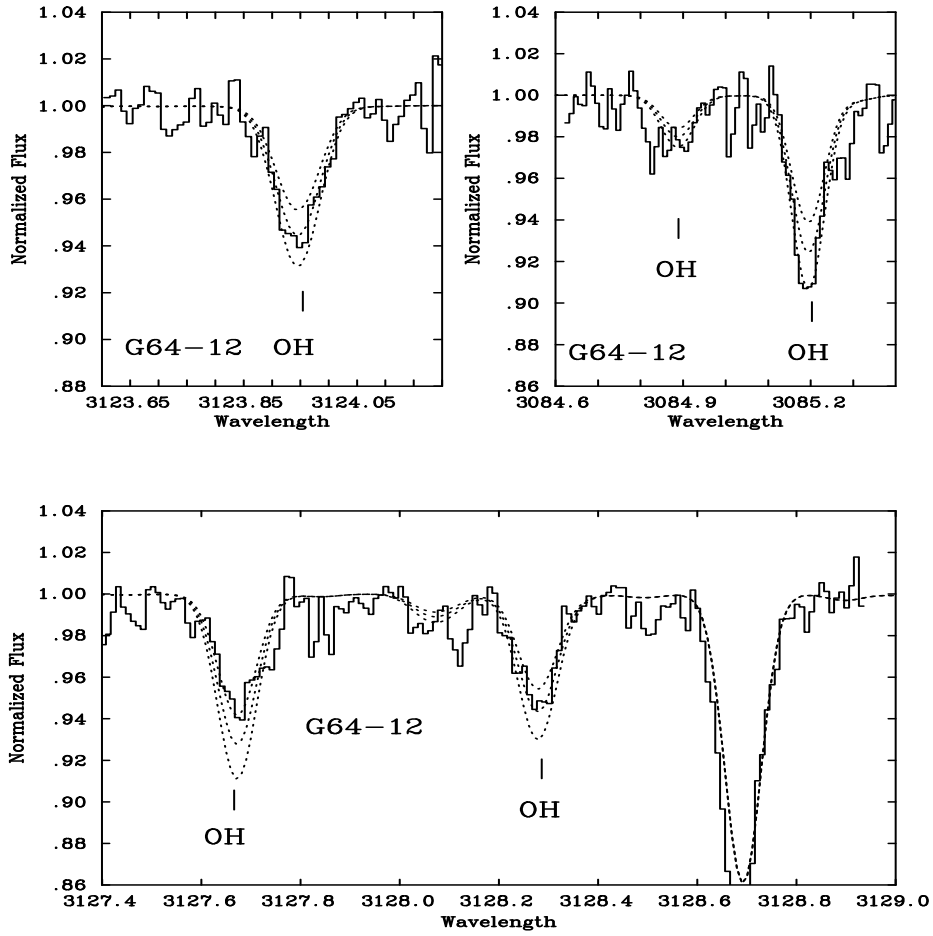


Fig. 3.— Synthetic spectra fits to the OH lines in the UVES spectrum of G64-12. The synthetic spectra are computed for  $\log \epsilon(\text{O})=6.95, 7.05$  and  $7.15$ .

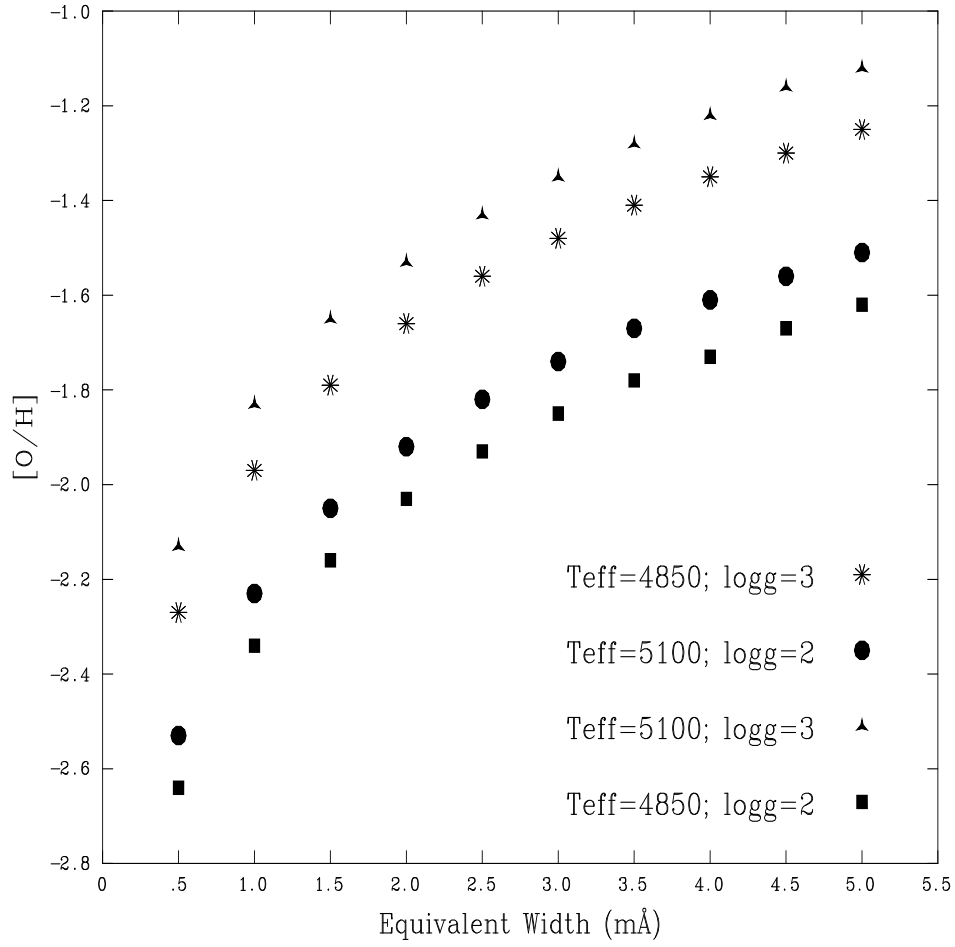


Fig. 4.— The oxygen abundance derived from the forbidden line [O I] 6300 Å for different values of the equivalent widths and four atmospheric models.

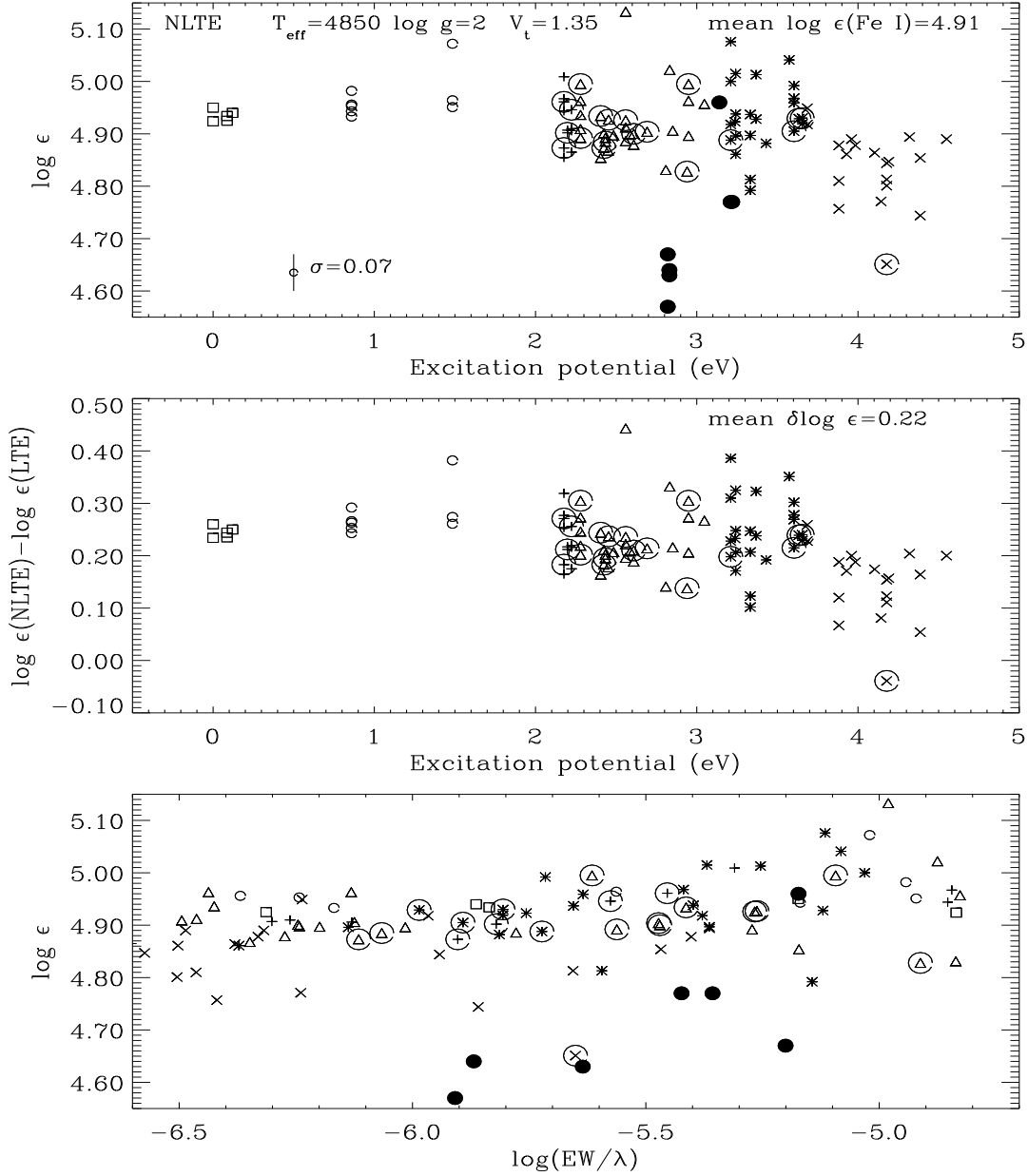


Fig. 5.— Results of NLTE abundance determinations for Fe I lines and model atmosphere with parameters  $T_{\text{eff}} = 4850$  K,  $\log g = 2.0$ ,  $V_t = 1.35$ ,  $\log \epsilon = 4.69$ . The lines with  $\chi < 0.8$  eV are marked as squares, the lines with  $0.8 < \chi < 1.8$  eV are marked as small unfilled circles, the lines with  $1.8 < \chi < 2.2$  eV are marked with pluses,  $2.2 < \chi < 3.0$  eV triangles,  $3 < \chi < 3.8$  eV are stars,  $3.8 < \chi < 4.8$  eV are crosses. The lines of Fe II are marked as filled circles. *Top*: NLTE abundances as a function of the lower excitation potential  $\chi$ . *Middle*: NLTE abundance corrections vs.  $\chi$ . *Bottom*: NLTE abundances as a function reduced equivalent widths  $\log(EW/\lambda)$ . The results for Fe I lines of different  $\chi$ -classes are denoted by different symbols. Fe I lines from the line list by Fulbright & Kraft 1999 are marked by large unfilled circles.

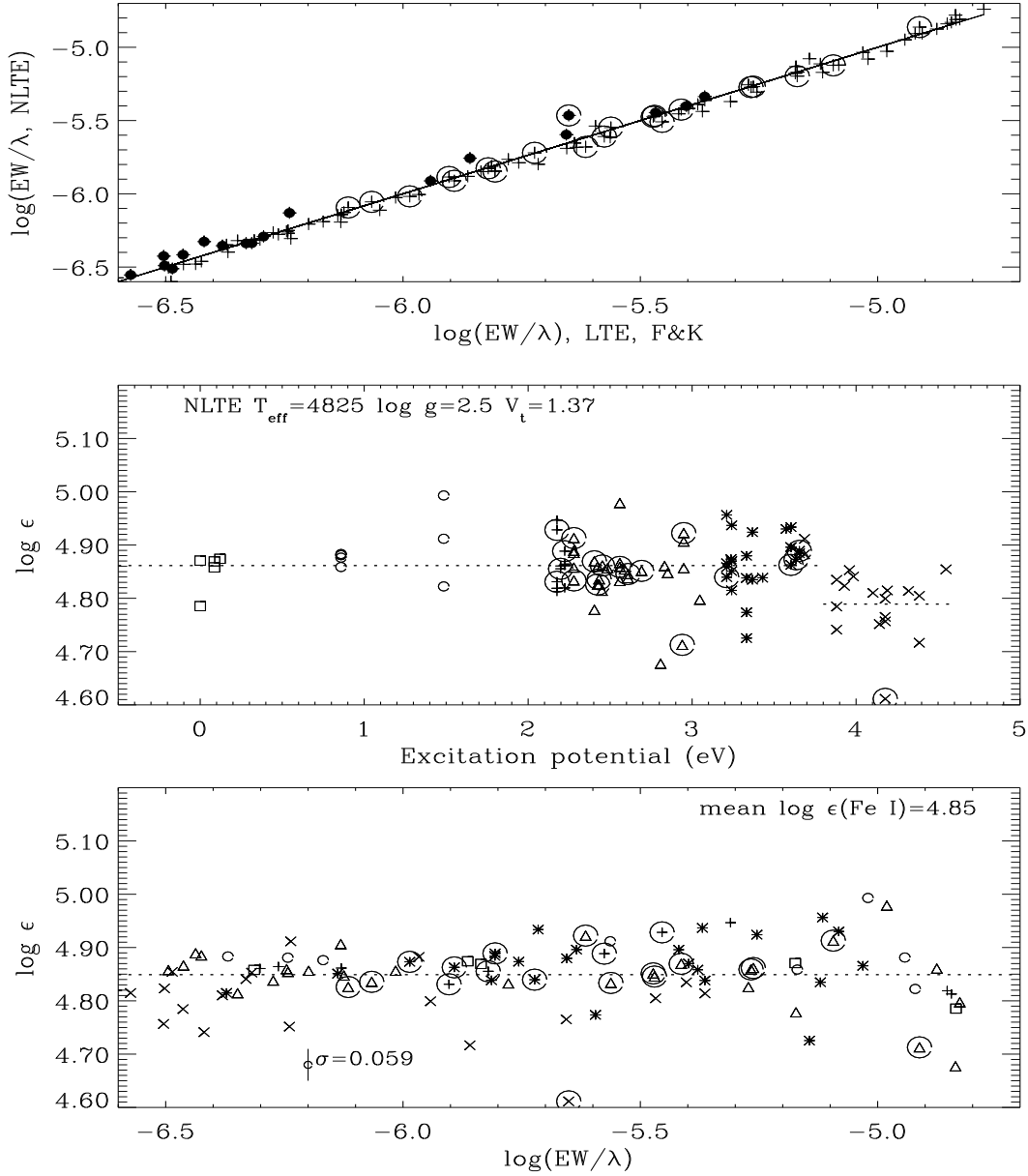


Fig. 6.— Computed equivalent widths  $\log EW/\lambda$  and NLTE abundances  $\log \epsilon$  for Fe I lines and for the parameters of the star BD + 23°3130:  $T_{\text{eff}} = 4825$  K,  $\log g = 2.5$ ,  $V_t = 1.37$ . *Top*: Computed NLTE equivalent widths for Fe I lines versus “quasi-observed” ones. The latter are calculated for the parameters found by Fullbright & Kraft (1999) using an LTE approach ( $T_{\text{eff}} = 4850$  K,  $\log g = 2.0$ ,  $V_t = 1.35$ ,  $\log \epsilon = 4.69$ ). The results for the high excitation lines are denoted by filled circles. *Middle*: NLTE abundances as a function of the lower excitation potential  $\chi$ . *Bottom*: The same values against  $\log(EW/\lambda)$ .

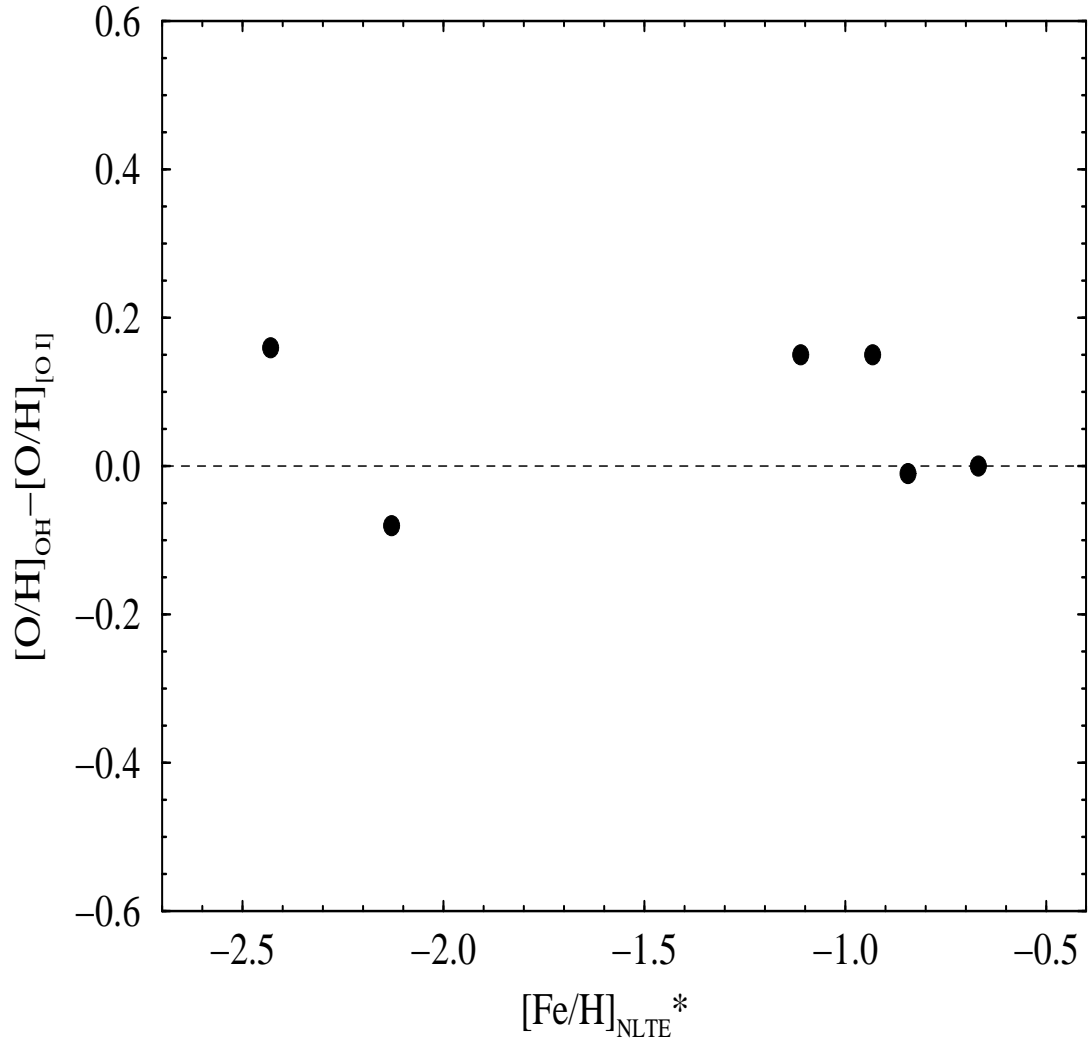


Fig. 7.— Differences between oxygen abundances derived from OH and forbidden lines for two stars discussed by FK and four stars from Israelian et al. (1998). The iron abundances have been corrected for NLTE effects as described in section 3.

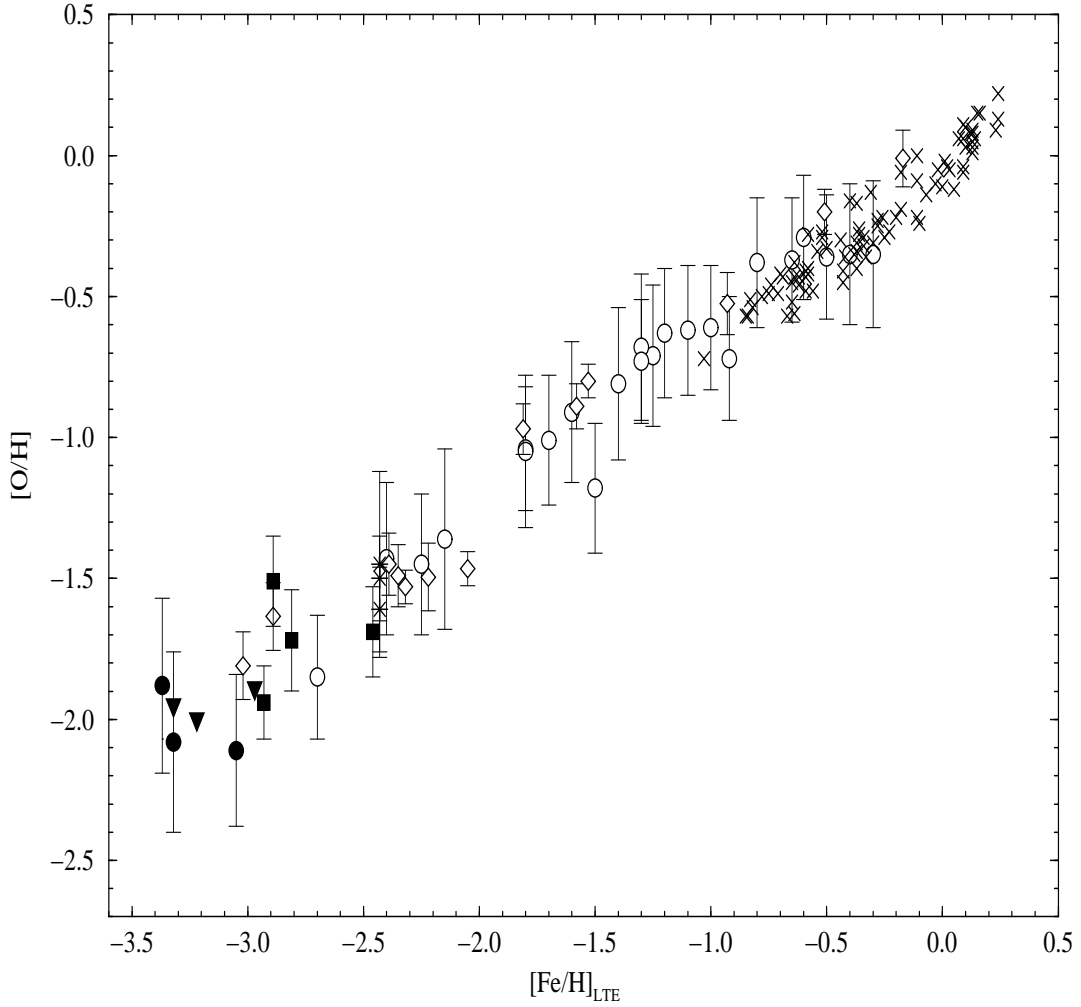


Fig. 8.— New oxygen abundances derived in this work together with those measured by Israelian et al., Boesgaard et al. and Edvardsson et al. (1993). The results for OH lines are denoted by filled circles, triplet by filled squares, and upper limits from triplet by filled triangles. The asterisks indicate the oxygen abundances derived from OH, triplet and  $[O\ I]$  for BD + 23°3130. Data from the papers of Israelian et al. (1998), Boesgaard et al. (1999a) and Edvardsson et al. (1993) are marked by unfilled circles, unfilled diamonds and crosses, respectively.

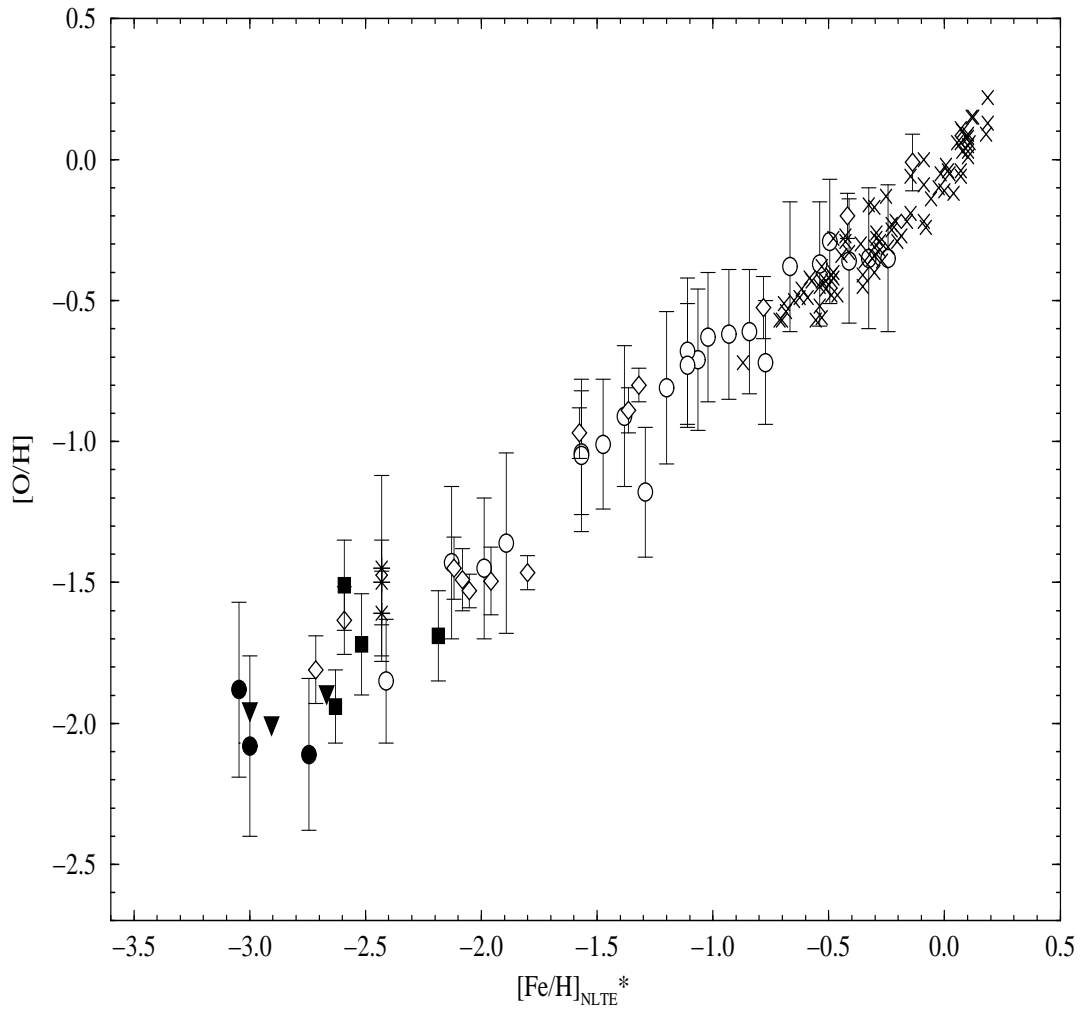


Fig. 9.— The same as in Fig 8. but with NLTE corrections estimated for  $[Fe/H]$ .

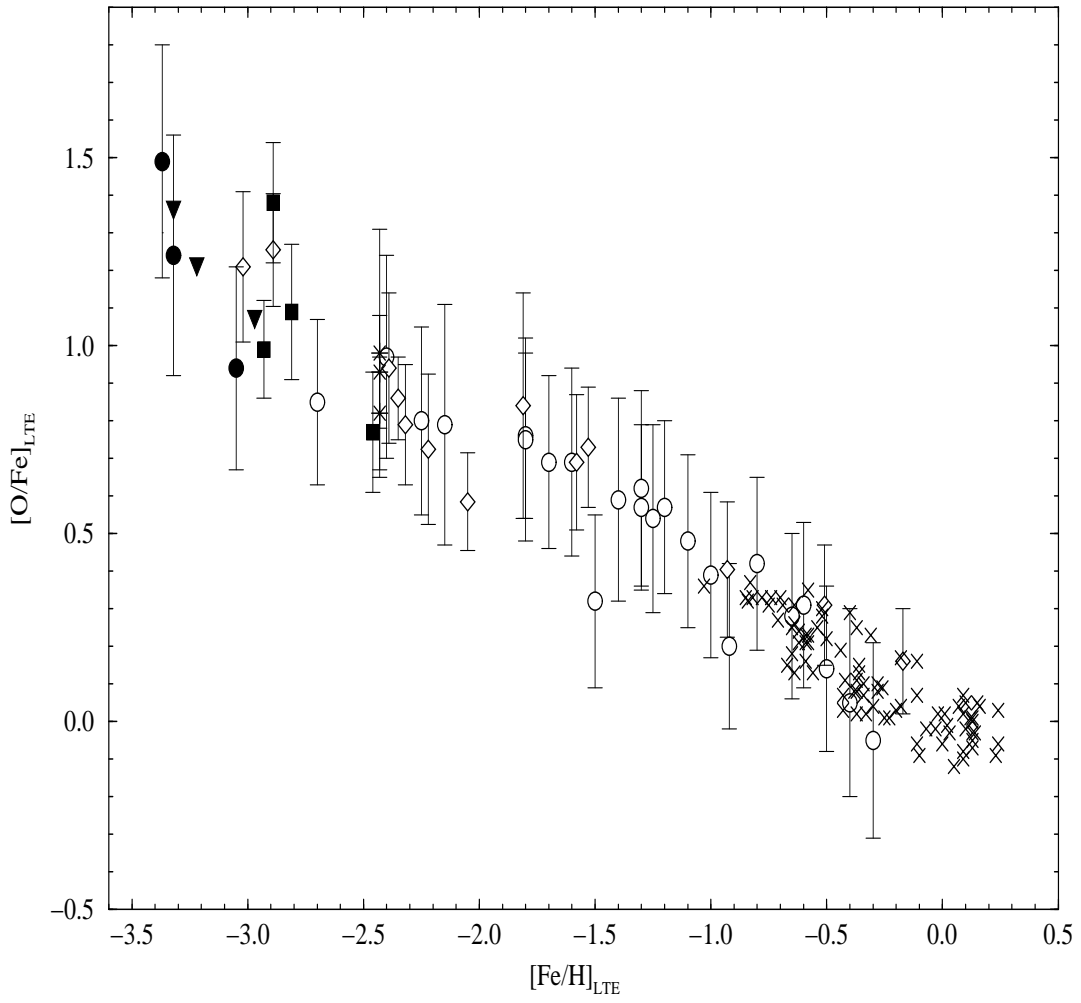


Fig. 10.— Oxygen overabundance with respect to iron, derived from the UV OH lines and the O I triplet in metal-poor unevolved stars. Symbols as in Fig 8.

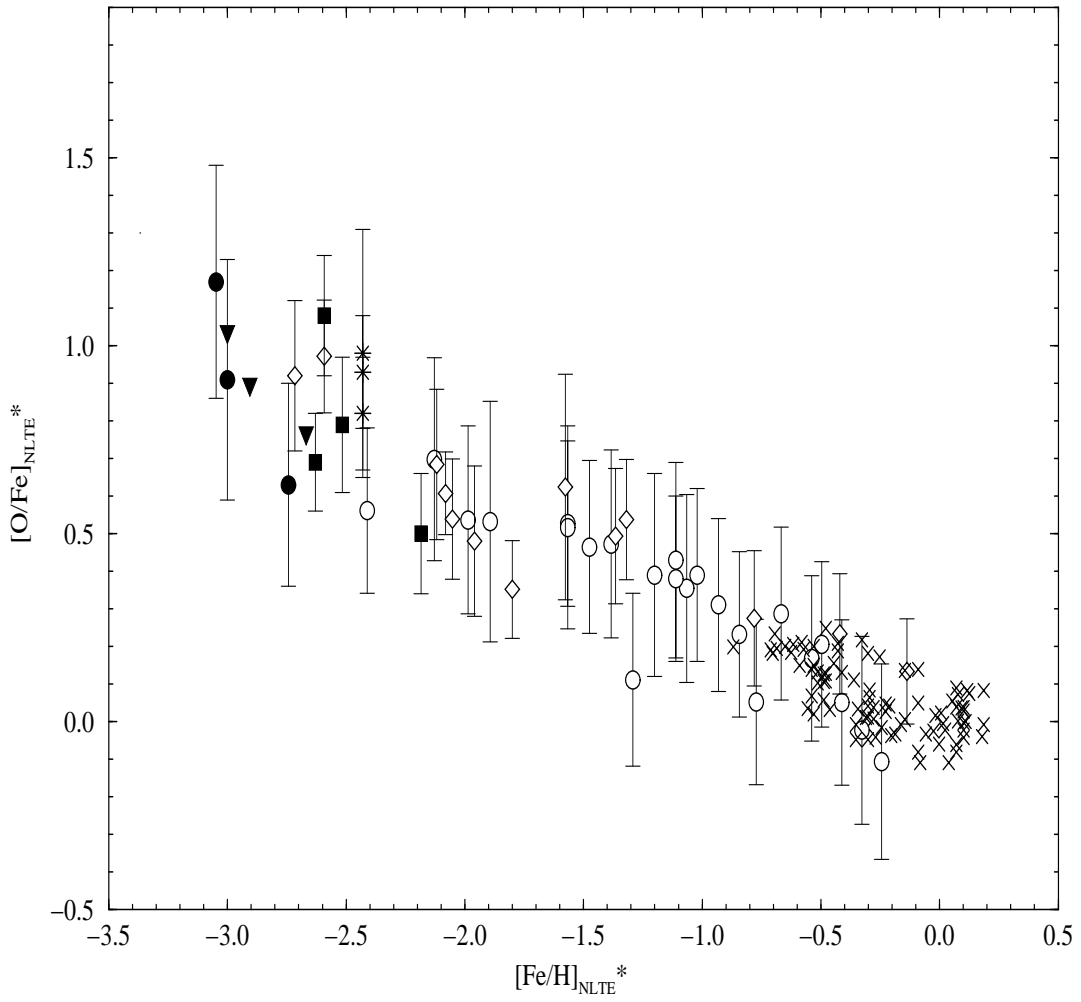


Fig. 11.— The same as in Fig 10 but with NLTE estimates of  $[\text{Fe}/\text{H}]$ .